

Review article

Inspiring a convergent engineering approach to measure and model the tissue microenvironment

Rishyashring R. Iyer^a, Catherine C. Applegate^{b,1}, Opeyemi H. Arogundade^{c,1}, Sushant Bangru^{d,1}, Ian C. Berg^{c,1}, Bashar Emon^{e,1}, Marilyn Porras-Gomez^{f,1}, Pei-Hsuan Hsieh^{c,1}, Yoon Jeong^{c,1}, Yongdeok Kim^{f,1}, Hailey J. Knox^{g,1}, Amir Ostadi Moghaddam^{e,1}, Carlos A. Renteria^{c,1}, Craig Richard^{c,1}, Ashlie Santaliz-Casiano^{b,1}, Sourya Sengupta^{a,1}, Jason Wang^{c,1}, Samantha G. Zambuto^{c,1}, Maria A. Zeballos^{c,1}, Marcia Pool^{c,i}, Rohit Bhargava^{a,c,e,g,h,i,j}, H. Rex Gaskins^{b,i,k,l,m,*}

^a Department of Electrical and Computer Engineering, University of Illinois Urbana-Champaign, Urbana, IL, 61801, USA

^b Division of Nutritional Sciences, University of Illinois Urbana-Champaign, Urbana, IL, 61801, USA

^c Department of Bioengineering, University of Illinois Urbana-Champaign, Urbana, IL, 61801, USA

^d Department of Biochemistry, University of Illinois Urbana-Champaign, Urbana, IL, 61801, USA

^e Department of Mechanical Science and Engineering, University of Illinois Urbana-Champaign, Urbana, IL, 61801, USA

^f Department of Materials Science and Engineering, University of Illinois Urbana-Champaign, Urbana, IL, 61801, USA

^g Department of Chemistry, University of Illinois Urbana-Champaign, Urbana, IL, 61801, USA

^h Department of Chemical and Biochemical Engineering, University of Illinois Urbana-Champaign, Urbana, IL, 61801, USA

ⁱ Cancer Center at Illinois, University of Illinois at Urbana-Champaign, Urbana, IL, 61801, USA

^j NIH/NIBIB P41 Center for Label-free Imaging and Multiscale Biophotonics (CLIMB), University of Illinois Urbana-Champaign, Urbana, IL, 61801, USA

^k Department of Animal Sciences, University of Illinois Urbana-Champaign, Urbana, IL, 61801, USA

^l Department of Biomedical and Translational Sciences, University of Illinois Urbana-Champaign, Urbana, IL, 61801, USA

^m Department of Pathobiology, University of Illinois Urbana-Champaign, Urbana, IL, 61801, USA

ARTICLE INFO

Keywords:

Bioengineering
Interdisciplinary research
Bioimaging
Biomaterials
Biosensing
Computational biology
Biomedical devices
Biotechnology

ABSTRACT

Understanding the molecular and physical complexity of the tissue microenvironment (TiME) in the context of its spatiotemporal organization has remained an enduring challenge. Recent advances in engineering and data science are now promising the ability to study the structure, functions, and dynamics of the TiME in unprecedented detail; however, many advances still occur in silos that rarely integrate information to study the TiME in its full detail. This review provides an integrative overview of the engineering principles underlying chemical, optical, electrical, mechanical, and computational science to probe, sense, model, and fabricate the TiME. In individual sections, we first summarize the underlying principles, capabilities, and scope of emerging technologies, the breakthrough discoveries enabled by each technology and recent, promising innovations. We provide perspectives on the potential of these advances in answering critical questions about the TiME and its role in various disease and developmental processes. Finally, we

* Corresponding author. Division of Nutritional Sciences, University of Illinois Urbana-Champaign, Urbana, IL, 61801, USA.

E-mail address: hgaskins@illinois.edu (H.R. Gaskins).

¹ These authors contributed equally and are listed alphabetically.

<https://doi.org/10.1016/j.heliyon.2024.e32546>

Received 16 February 2024; Received in revised form 22 May 2024; Accepted 5 June 2024

Available online 8 June 2024

2405-8440/© 2024 The Authors. Published by Elsevier Ltd. This is an open access article under the CC BY-NC license (<http://creativecommons.org/licenses/by-nc/4.0/>).

present an integrative view that appreciates the major scientific and educational aspects in the study of the TiME.

1. Introduction

The structure and composition of human tissues is spatially and temporally expansive. Typically, a specific cell type (for example, epithelial cells in breast tissue) comprises the key functional element of the organ and several other cells and extracellular materials provide structural and operational support. Collectively, they form the tissue microenvironment (TiME). Important length scales in the microenvironment span over ten orders of magnitude, from single molecules that are a few nanometres in size to the entire human body that spans a couple of meters. From an engineering perspective, the structure, function, and dynamics of the TiME are not only the zenith of system complexity but also an aspirational goal to mimic, monitor, and modify. Researchers usually employ one of two strategies to tackle this complexity. The top-down approach, in which the response of the entire system to a targeted stimulus is observed, has been historically prevalent since it relies on natural observation. However, this approach offers only a limited understanding of the many processes that determine overall response. A bottom-up approach involves breaking down the system into its fundamentals and studying them individually. However, such an approach is technically challenging since it requires a high degree of control in stimulation, specificity in observation, and versatility in application whereas translation of results to whole systems is less assured. In addition to these complexities of spatial heterogeneity across scales, the role of the TiME often needs to include an understanding of the mechanical, biochemical, and electrical properties.

For example, consider the microenvironment of the human eye. In the retina, there are unique light-matter interactions between the photosensitive cells in the retina in which conformity of the opsins, photosensitive molecules, are changed in response to light. This biochemical reaction induces electrical activity in these cells. However, the process of vision relies on the computational preprocessing at the millisecond scale that happens in retinal ganglion cells and the various cells that support its functionality. Besides complex visual processing, on a slightly larger scale, the preprocessing in the retina also induces the mechanical functionalities of the human eye to track and focus on motion or objects of interest by moving the ocular muscles through neuromuscular junctions. At the same time, on a macro scale, there exists constant communication between the eye and the brain, both for vision on shorter time scales and for regulating the light-based circadian rhythm on a longer time scale. While it is indeed difficult to study such a complex system with ease, emerging approaches to record and parse data are now making it possible to study TiME-function relationships with both top-down and bottom-up approaches. The purpose of this review is to introduce the reader to an integrated framework for sensing, analysing, modelling, and understanding the TiME.

We illustrate the elements of an integrated approach in Fig. 1. Here we show two examples of a physiologic intervention to understand function (left) and its use to study disease progression (right), highlighting the opportunity of an integrated approach to study

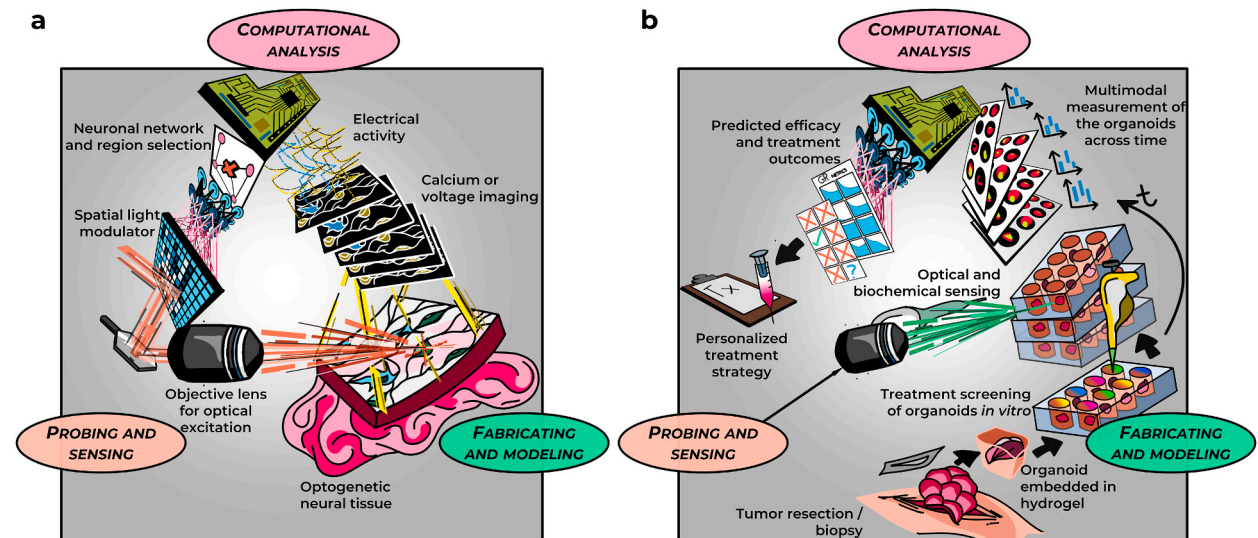


Fig. 1. An integrated framework to study the tissue microenvironment. We organize integrated studies into 3 broad fields. First, probing and sensing technologies focus on harnessing recent advances in microelectronics optics and fabrication to provide unprecedented level of detail and amount of data. Second, recent advances in microfabrication and manufacturing offer new opportunities to model and make representative versions of the TiME. Finally, the enormous increase in capability of computing, storage and communication resources in recent years makes it feasible to utilize the data from model systems under a large variety of conditions. Together, these three trends allow for a convergent approach to study the TiME. **a-b.** Here we present an overview of selected, key technologies that can be used in the same overall framework to study the role of the TiME in (left) physiologic neuronal responses, and (right) in cancer progression.

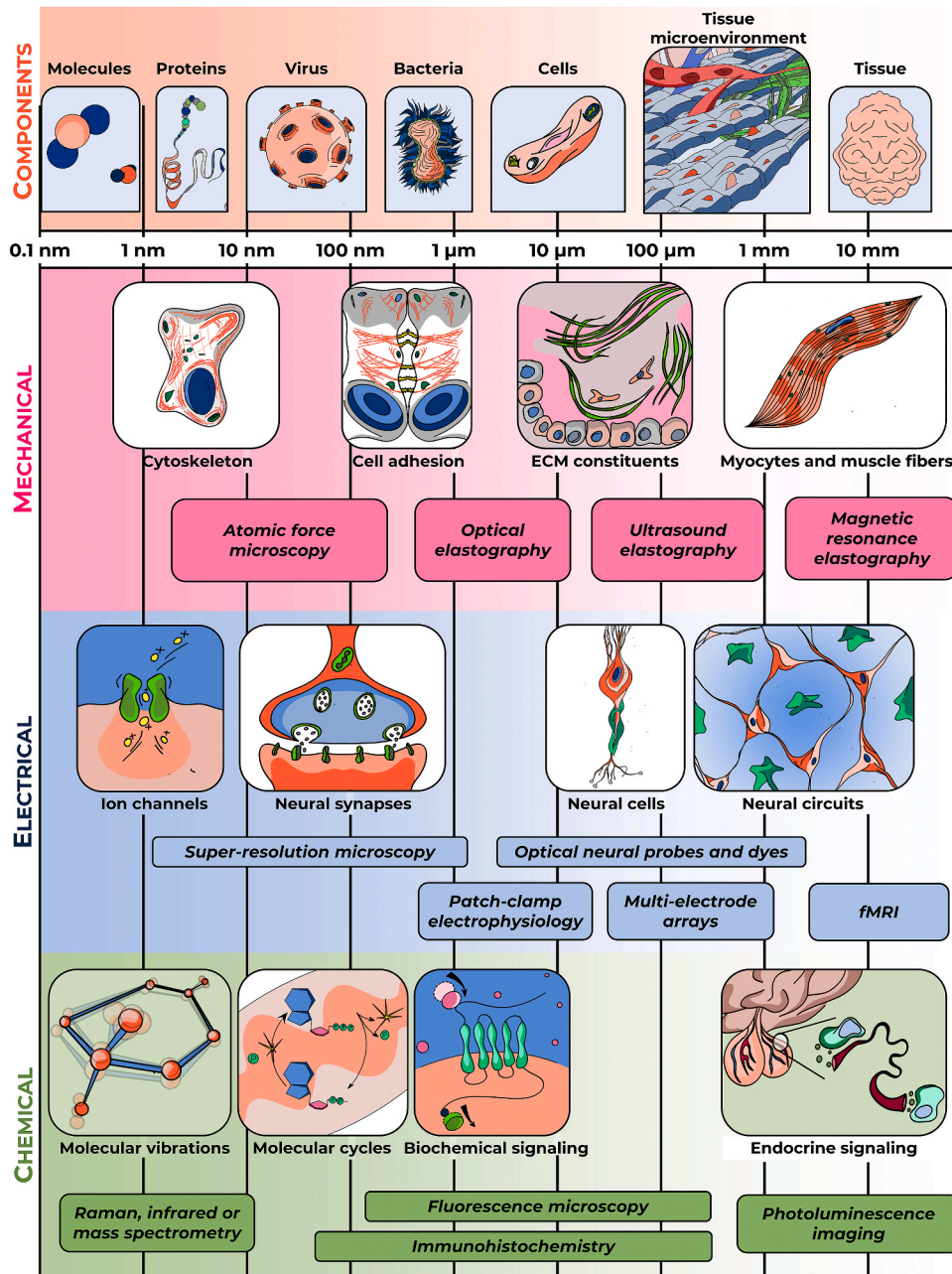
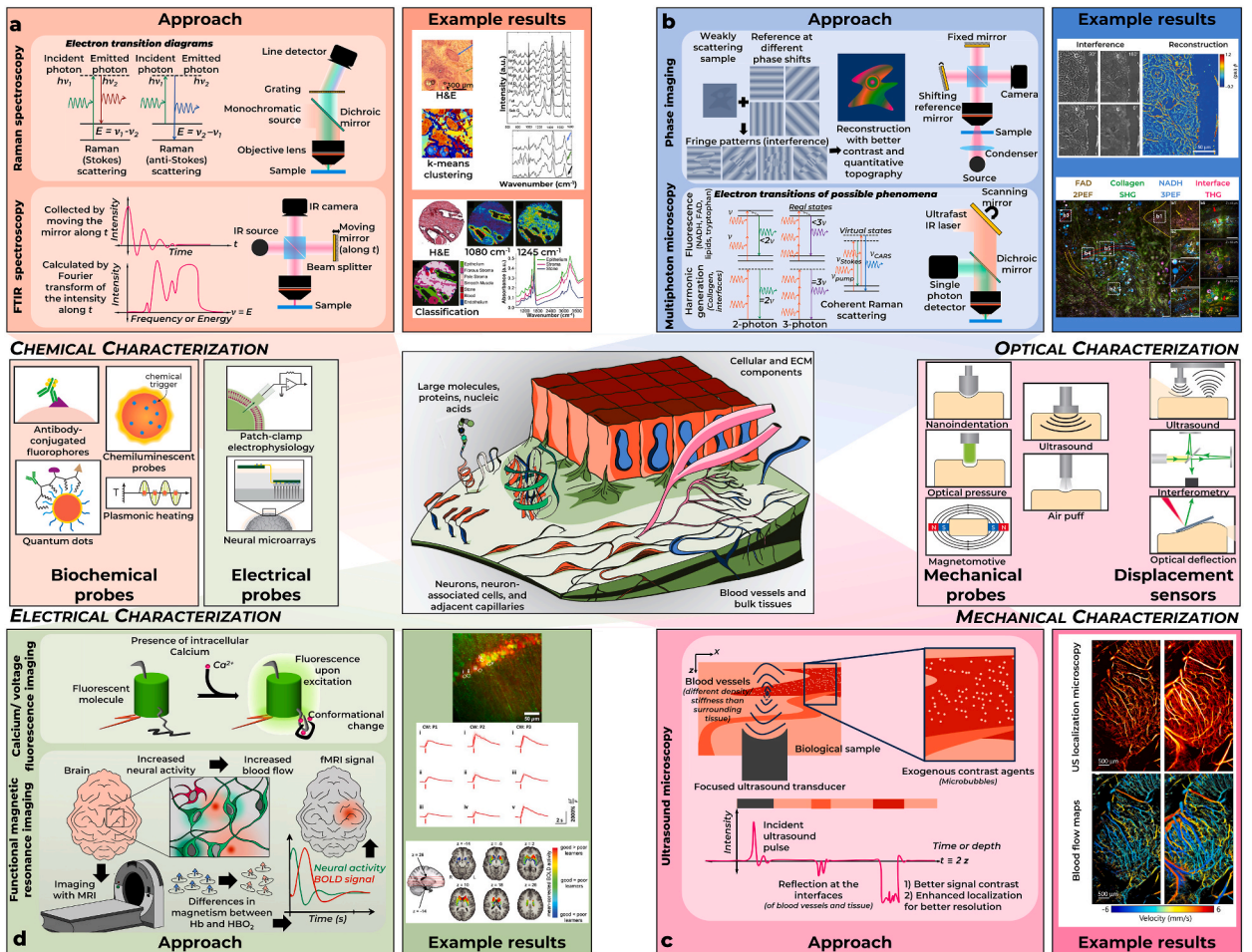


Fig. 2. Length scales of the tissue microenvironment processes and methodologies. The different rows describe the components of the tissue microenvironment at their approximate spatial scales, and biological phenomena broadly categorized as mechanical, electrical, or chemical processes from the top to the bottom. Among the mechanical phenomena, the cytoskeletal tension from actin (dark orange) and microtubules (light orange) which are 5–25 nm thick, the adherens junctions between epithelial cells (200–800 nm long, 20–50 nm wide) tethered by the actin molecules (orange filaments), the extracellular matrix (ECM) constituent proteins such as collagen (green strands) that constitute the tissue bulk on the microscale (10–100 μm), and the muscle cells and fibres that can span several millimetres are described from the left to right. Among the electrical phenomena, the ion channels (<0.2 nm) that allow K^+ , Na^+ , Ca^{2+} transmission on a millisecond-scale, neural synapse with synaptic vesicles (<50 nm) and the neural cleft (the gap in the junction, 20–40 nm), a neural cell with a long axon wrapped in myelin (cyan), the round soma, and the dendritic projections (top), and a neural circuit with interconnected neurons (orange) and supporting glial cells (cyan) are illustrated from the left to right. Among the chemical phenomena, the molecular vibrations on a sub-nanometre scale, the molecular cycle of ATP-ADP that happens inside a mitochondrion (500–1000 nm), biochemical signalling through a transmembrane receptor, and endocrine signalling that happens across several meters through the vascular pathway are illustrated. (For interpretation of the references to colour in this figure legend, the reader is referred to the Web version of this article.)



(caption on next page)

Fig. 3. Overview of the approach and example results of the techniques for probing and sensing TiME properties. (Centre) Increasing length scales of the components of TiME from top left corner to the bottom right corner encompassing characterization of chemical, optical, electrical, and mechanical properties.

a. Chemical characterization: (Top) Approach of Raman spectroscopy describing the electron transition diagrams (Jablonski diagram) for Stokes and anti-Stokes Raman scattering where the absorption of a photon induces the electron to transition to a virtual electronic state before falling to the ground state. The accompanying system diagram describes a typical Raman spectroscopy setup in epi detection mode. The accompanying images show its application in breast-cancer detection, adapted from Ref. [1]. (Bottom) Approach of FTIR spectroscopy showing the system setup for interferometric detection of absorbance, typical signals in the TiME domain for each pixel and the extraction of the spectroscopic characteristics by a time-to-frequency Fourier transform. The images on the right show a typical H&E image typically used in histopathology reregistered with the FTIR image at two selected wavelengths for a sample of prostate cancer. The graph shows the average spectra from selected regions in the sample corresponding to epithelium, stroma, and stone. Based on the spectra and spatial features, FTIR can be used to detect and classify different components of TiME. Adapted from Ref. [2].

The box contains a few biochemical probes for targeted labelling of tissues using the ubiquitous antibody conjugated fluorescence proteins, quantum dots that enhance the fluorescence of typical fluorophores, chemiluminescent probes for live whole-body imaging, and plasmonic heating for localized thermal excitation.

b. Optical characterization: (Top) Approach of phase imaging describing a typical setup capture the self-interference at different phase shifts, corresponding images before and after interference at four different phase shifts 90° apart. The example results depict an image of neuronal cells grown on a coverslip captured by GLIM at four phase shifts and reconstruction of quantitative optical phase from these images, adapted from Ref. [3]. Scale bar: 50 μm . (Bottom) Electron transition diagram for various nonlinear light-matter interactions and the relationship between excitation and emission frequencies. Typical system setup of multiphoton microscopy showing an ultrafast NIR light source (centred around 700–1200 nm, 20–50 nm bandwidth, <200 fs), dichroic mirrors and filters, high-numerical objective lenses (>0.8 NA), and single photon detectors (such as photomultiplier tubes, hybrid photodetectors, electron-multiplied charged coupled devices, or avalanche photodiodes). The image on the right shows the multimodal nonlinear label-free image of a breast tumour in rats captured *in vivo* in a multiphoton setup with four multiplexed detectors excited with a 60-fs source centred at 1110 nm capable of imaging signals from NAD(P)H (3-photon excitation fluorescence or 3PEF), FAD (2-photon excitation fluorescence or 2PEF), collagen (second harmonic generation or SHG), and bilipid interfaces (third harmonic generator or THG) simultaneously, which are found in various components of TiME, adapted from Ref. [4]. Scale bar: 100 μm .

c. Mechanical characterization: Approach of ultrasound localization microscopy where microbubbles used as exogenous contrast agents into blood vessels are imaged with ultrasound microscopy for enhanced contrast and localization by the decorrelation of highly reflective microbubbles within microvasculature. A representative image of ultrasound super-resolution localization microscopy of mouse brain and corresponding doppler image showing the velocity of blood flow through the microvasculature, adapted from Ref. [5]. Scale bar: 100 μm .

The box contains approaches for exerting stress (left) and measuring the strain (right) for probing the mechanical properties of biological samples. Nanoindentation with optical deflection comprises atomic force microscopy; optical pressure, ultrasound, or magnetomotive forces with low coherence interferometry comprise photonic force, acoustic radiation force, or magnetomotive optical coherence elastography techniques; ultrasound or air-puff excitation with ultrasonic detection comprises ultrasound elastography.

d. Electrical characterization: (Top) Approach of using fluorescent tags for imaging ion flux or membrane potential differences into a cell, typically a neuron at millisecond-to-seconds scale, where the fluorescent molecule undergoes conformational changes upon binding to Ca^{2+} ions and becomes fluorescent upon excitation with visible light. The images on the right show the average fluorescence from GCaMP6s frames of a neural cell culture with traces from certain regions in the sample [6]. (Bottom). Approach of fMRI to capture the vascular dynamics resulting from neural activity in certain regions in the sample by harnessing the differences in the magnetism of oxygenated and deoxygenated blood creating contrast when imaged serially using MRI using a technique called Blood-oxygen-level-dependent imaging. The images on the right correspond to fMRI images captured for different learners for a task at different depths in the brain, adapted from Ref. [7].

The box contains schematics for patch clamp electrophysiology (traditional method to measure the electrical activity of neurons) and neural microarrays that can be implanted in the skull semi-permanently to continuously monitor electrical signals over a region along the brain surface and transmit data wirelessly.

diverse systems and phenomena of importance. One pillar of our approach is probing and sensing. Fig. 2 describes the various constituents of the TiME across length scales that span both top-down and bottom-up studies. At each scale, we highlight key functionalities and sensing techniques useful to investigate these properties. Our review is partly motivated by providing the reader with an overview of each since multimodal approaches will surely be needed to probe TiME's spatial and compositional complexities. The rise in sensing capability is highly synergistic with recent advances in computational capabilities; this interaction enables more sophisticated analyses that drive the need for even more computing complexity. Thus, computational analyses that leverage multiscale and multidimensional datasets to address the TiME's spatiotemporal complexity with modern modelling need to be integrated as a second pillar. Finally, advances in manufacturing and microfabrication are providing new opportunities to develop models of the microenvironment and perturbations to function. While advances in each of these areas can advance our understanding of the TiME, their integration in a convergent approach can be more powerful.

This article seeks to introduce the key elements of each of these three pillars of a convergent approach. It summarizes the forefront of technologies and technical advances in probing and sensing in Section 2, modelling and fabricating TiME in Section 3, and computing in Section 4, directed primarily for early-career researchers in this field. Our goal is to provide basic knowledge, key references and avenues for future studies and development. The technologies have been categorized based on underlying engineering principles. These classifications were made only to organize these techniques and not a strict definition of their principles; some of them discussed could belong to several categories. Each section outlines the underlying principles, the capabilities, and scope of the current technology, the breakthrough discoveries enabled by the technology, the recent innovations in the technique, and its potential to address unanswered and underexplored questions about TiME. Finally, Section 5 highlights applications of the techniques in Sections 2-4 towards integrative approaches for studying the neuronal and cancer microenvironments. Finally, we discuss successful

translations of such studies into the clinical environment to underscore the impact of using an engineering approach in TiME studies to advance healthcare.

52-4

2. Probing and sensing time

Our understanding of TiME has relied upon the centuries-long development in technologies that can probe and sense various components. Historically, these techniques relied upon our visual or tactile perception of TiME through optical imaging and palpation, respectively. However, these are but a small subset of physical properties that describe TiME. This section describes how the principles of different disciplines of engineering have been used to sense and probe (Fig. 3) the chemical, material, optical, and mechanical properties of TiME. We have focused particularly on three aspects of these techniques: improvements in their specificity (such as novel targeted fluorescent or chemiluminescent tags and advanced spectroscopic techniques), reducing their degree of invasiveness (such as label-free optical microscopy and non-contact ultrasound elastography), and expanding their dimensionality (such as multimodal imaging techniques and AI-enabled image-to-image translation techniques).

Sensing the chemical properties often involves trying to decipher the molecular composition of the TiME by estimating the energy of the molecular bonds in the sample, often utilizing the interactions between the material and an electromagnetic field (light, X-rays, ions). The probing aspect of these principles typically involves the design of materials according to some unmet need. A relatively recent development in materials engineering is the design and application of nanomaterials, whose functional dimensions lie between 1 and 100 nm. A key aspect of nanomaterials is the emergent properties that arise from the nano structuring of a material that are often not present in the bulk material. These principles have been used in the development of novel tags and probes for tissue microenvironments such as localized heating, localized magnetic fields, and amplified fluorescence (Fig. 3a). Apart from these probes, light-matter interactions in the TiME have been used to sense a wide range of physical, chemical, and biological properties at a micron-scale. Even though light has limited penetration within tissues (typically a few hundred microns, sometimes up to a few millimetres), the wavelength of light and its relatively non-destructive nature makes it ideal for observing the TiME at the relevant scales. Light-matter interactions can be categorized into linear (where the wavelengths of the excitation and emitted light are the same) and nonlinear (where the wavelength of excitation and emitted light are different) phenomena. The former, typically referred to as scattering, is used in both fundamental techniques such as the ubiquitous brightfield microscopy and advanced precise techniques such as quantitative phase imaging and optical coherence microscopy. The latter is used to observe specific components of the TiME, such as metabolites, lipids, or proteins, by observing their specific nonlinear interactions with light. Discussing the entire realm of optical engineering in the life sciences and the centuries-long progress in the fields of quantum-physics, instrumentation, genetic engineering, and bioinformatics is beyond the scope of this paper. Therefore, we have focused on the progress in sensing TiME components label-free, concentrating on the innate interactions between light and TiME and not on the use of exogenous agents such as fluorescent, luminescent, or spectroscopic tags. Fig. 3b illustrates the principles and example results of a few popular label-free imaging techniques.

Probing the mechanical properties at the macro scale has been a widely used metric in the clinical sciences starting from simple tests such as palpating for lumps as an early detection of cancer to quantitative measures such as intraocular pressure. On a micron scale, measuring the mechanical properties is crucial to analysing the progress and pathology of these techniques. Also, the contrast in mechanical properties of different TiME components not only enables mechanical imaging techniques such as ultrasound microscopy, but also enables accurate characterization of critical processes such as cell adhesion, protein tethering, cell-ECM interactions, and blood-flow dynamics (Fig. 3c). The role of electrical engineering in TiME falls under two broad categories: techniques that sense interactions between TiME components and external electromagnetic fields (excluding light) and techniques that treat the electrically active TiME components as a part of the circuit. The former is popularly used in clinical environments via techniques like magnetic resonance imaging, the latter forms fundamental tools in neurosciences. We have focused particularly on techniques that expand the functionality and dimensionality of these techniques (Fig. 3d).

2.1. RAMAN, FTIR IMAGING AND SPECTROSCOPY

Vibrational spectroscopies, which include Raman spectroscopy and mid-infrared (IR) spectroscopy, directly measure the chemical bonds present in samples [8]. Raman spectroscopy measures a material's response to light based on the polarizability of bonds within its molecules. Light excitation causes the formation of an excited virtual energy state, the relaxation from which results in the emission of photons with an energy difference between the final and initial states. This difference can be measured by using any wavelength of light to excite the molecular bond and each type of bond provides a different shift, thereby allowing a fingerprinting of the molecular composition. Infrared spectroscopy, in contrast, measures a quantity related to the inherent dipole moment of molecules with IR frequencies being absorbed by chemical bonds at their resonant frequency. This resonant frequency is related to the strength of the bond and the mass of the atoms involved in that bond whereas the fraction of light absorbed is related to their concentration in the sample, thereby allowing a direct optical recording of the chemical composition [9].

Full IR spectra are typically measured using Fourier transform infrared (FT-IR) spectroscopy and spatially resolved spectroscopy, i. e. FT-IR imaging [10], has been used to probe the structure of the microenvironment of many tissues [11]. Using the chemical composition of cells and their physiology as a fingerprint [12], IR spectra can be combined with artificial intelligence to understand composition and the role of the TiME in disease progression [13]. IR spectroscopy can measure "meso-scale" chemical compositions, generally providing total protein, lipid, carbohydrate, nucleic acid and metabolite concentrations; however, greater details may be available in some instances such as probing secondary protein structure [14–16] (e.g., alpha helix, beta pleated sheet, random coil) or

specific DNA peaks [17,18]. IR imaging with quantum cascade lasers (QCLs) [19,20] has greatly improved imaging speed and resolution to enable high-throughput, high-fidelity characterization of tissue samples. Novel sensing techniques are now expanding the applicability of IR imaging [21,22] to theoretically optimal and beyond the diffraction limit [23,24]. Given the strong absorption of light, measurements of aqueous and thick sections of tissues are difficult.

Since polarizability of water is low and the Raman effect is weak, Raman spectroscopy is relatively insensitive to water. Moreover, the ability to use different wavelengths and linear and nonlinear processes allows for deep tissue, sensitive and high-resolution measurements. While the process of spontaneous Raman scattering is intrinsically weak and, consequently, slow, coherent Raman scattering processes have been harnessed to develop stimulated Raman scattering (SRS) [25,26], surface-emission Raman scattering (SERS) [27,28], and coherent anti-Stokes Raman scattering (CARS) microscopy [29,30] techniques. Current research in Raman spectroscopy has focused on novel methods to accelerate the speed of imaging such as rapidly tuneable coherent laser sources, spectrally tailored broad-band sources [31], and spectral-temporal focusing [32], all while maintaining the spatial and spectral resolution necessary for probing the molecular content and heterogeneity in the TiME. Further research in improving the interpretability of the spectroscopic images for biologists, improving the information efficiency, developing IR or Raman tags in the “silent” vibrational spectral regions [33–39] for improving the specificity of imaging, and adapting these techniques for biomedical diagnosis through computational imaging techniques can improve the ubiquity of label-free spectroscopy for probing the TiME.

2.2. PLASMONICS

Metallic nanoparticles exhibit oscillations in the electron density at their surface, which are called localized surface plasmons. Incoming light excites these oscillations and light that matches the frequency of these oscillations maximally induces this localized surface plasmon resonance. Joule heating from the increased electron movement coupling to lattice vibrations can cause nanoparticles to rapidly heat their local environment [40–43]. These properties can be leveraged as cancer treatments with photothermal therapies. Targeted nanoparticles are injected and accumulate in the tumour. Near infrared (NIR) light or radio can then be used to excite localized surface plasmon resonance (LSPR), heating the particles and the cancer cells as well as TiME cells in their vicinity [44]. Depending on the intensity and temporal delivery and temperatures achieved, this induces cell death through protein denaturation, edema, and necrosis. LSPR generation in biological samples have also been utilized for sensing molecular interactions [45,46], controlling fluorescence dynamics [47], light-induced therapeutics [48,49], and detecting cancer biomarkers [50].

2.3. NOVEL BIOCOMPATIBLE TAGS FOR IMAGING

Utilizing “dyes” such as indigo, saffron, or madder root to visualize biological samples has existed since the invention of the microscope [51] in the 18th century. Thereafter, research has focused on improving the specificity of these labels and efficacy of delivery into biological samples. Traditionally, fluorescence microscopy is dependent on popular tags such as engineered green fluorescent proteins [52], quantum dots [53,54], and viral transfection mechanisms. However, recent work has also focused on developing tags for spectroscopy (e.g., deuterated molecules [33–35], metal carbonyls [36,37], and azides [38,39] in the silent regions of vibrational spectroscopy), scattering-based techniques (e.g., gold nanoparticles [55,56]), and photoacoustic microscopy (e.g., microbubbles). The specificity is controlled in two domains – spatial localization and component specificity. The former is typically controlled by the delivery mechanism by carrier like nanoparticles [54], silicon [57–59] or carbon shells [60,61], and nano motorized carriers [62,63]. Popular techniques include matching the sizes of the carrier and pores or channels in the tissue. These carriers not only enable localization, but also amplify emitted signal levels to improve imaging efficiency. Methods for component targeting include antibody-conjugation, genetic engineering and transfections [64]. A list of reactive small molecules [65] that fluoresce upon activation while being permeable through most biological barriers have been utilized to probe key biomolecular relationships and organelles even at a sub-cellular level [66]. Tags have also been developed to measure the properties of the local microenvironment such as temperature [61], oxygen levels [67] or local enzymatic activity [68]. Another popular candidate are the nanodiamonds [69] with nitrogen vacancies, whose fluorescence is dependent on magnetic fields, that have been used as temperature [70] and biomechanical sensors [71]. Current research has focused on improving the dimensionality and efficacy of these tags to avoid the spectral crowding of biological peaks and molecules of interest. To improve the limit of detection on the instrument, researchers have introduced bi-orthogonal tags or labels [72,73] on the backbone of targeted molecules and localized to the surface or interior of nanoparticles. Techniques such as PICASSO [74] and DNA-PAINT [75] have utilized novel tags coupled with computational imaging techniques to generate highly multiplexed tags that provide highly specific multidimensional profiles of TiME. Extending these for *in vivo* and dynamic imaging with minimal invasiveness can drive further progress in our understanding of TiME.

2.4. LABEL-FREE PHASE IMAGING AND INTERFEROMETRIC TOMOGRAPHY

The differences in the scattering profiles of biological samples from its environment, although very subtle, was among the first known contrast in light microscopy [76–78]. Precisely, these differences arise from the local heterogeneity in the refractive indices. There have been two methods to maximize these subtle differences: holography [79,80]/phase imaging [3] and interferometry [81]. Both methods rely on enhancing the contrast by observing the differences in the sample with respect to a reference. While the former uses a self reference, typically the low-spatial-frequency components in the sample, the latter typically uses a mirror in a separate beam path as its reference. Recent progress in phase imaging has been to extract the quantitative optical phase from the samples, from which parameters such as the dry mass [82,83], refractive index [84], axial profile [85], and ion flux [86,87], have been estimated. Popular

techniques in phase imaging include digital holographic imaging, spatial light interference microscopy (SLIM) [88], and gradient light interference microscopy (GLIM) [89], where a series of images are acquired with different phase differences between the sample and reference for quantitative reconstruction. A disadvantage of phase imaging is that it is limited to imaging thin samples ($\sim 1 \mu\text{m}$). Optical interferometric techniques such as optical coherence tomography (OCT) and microscopy (OCM) cause amplification of the backscattered signal through low coherence interferometry, often up to 80–100 dB. Using low-coherence light, i.e., spectrally broadband light, in interferometry ensures intrinsic axial sectioning in the sample due to the low coherence length of these sources. Intrinsic axial sectioning and analysis in the Fourier space also ensures 3D imaging capabilities.

Both OCT and phase imaging have been successfully commercialized over the last two decades for biological and clinical imaging [3,90,91]. Especially, OCT has found ubiquity in ocular imaging due to its ability to image the different layers of the human eye, including the retina [92], precisely and fast. Besides an effort to expand the commercial applications of these techniques, researchers have focused on extracting functional contrast [93] such as blood oxygenation levels [94], mechanical properties [95], tissue birefringence [96,97] to quantify the biological dynamics such as blood flow, tissue viscoelasticity, or fibre orientation of TiME.

2.5. LABEL-FREE MULTIPHOTON MICROSCOPY

The wavelength of the excitation and emitted light are the same in phase imaging and OCT/OCM. However, there are several light-matter interactions in which the emitted wavelength differs from the excitation wavelength [98], among which fluorescence is a popular example. There are several autofluorescent molecules in tissues, such as NAD(P)H, FAD, lipids, tryptophan, and porphyrins, that not only highlight tissue components but also inform their metabolic states [99–101]. While the spectral overlap in traditional confocal or single-photon fluorescence imaging may be limited, multiphoton microscopy using ultrashort laser pulses [102–104] can create a greater degree of separation between excitation and emission spectra. Multiphoton nonlinear imaging can also unlock new contrasts such as harmonic generation (in which the emitted frequency is an exact multiple of the excitation frequency), which can probe TiME components like collagen and bilipid layers easily [105–107]. Similar multiphoton nonlinear processes have been utilized for coherent Raman spectroscopy (described in section 2.1). The large spectral separation between these phenomena also facilitates easy multiplexing of these phenomena into the same setup with a single source [4,108]. Current efforts in this field have focused on improving the functional utility of these techniques to extract parameters such as fluorescence lifetime [109] and Förster resonance energy transfer by improving the excitation technology with spectral tailoring of ultrashort broadband pulses [110] and integrated high-speed electronics in the digitizer [111,112]. These technical improvements have also led to accelerated research on improving the specificity and increasing the multimodality [4,113–115], where several contrast mechanisms could be accessed at once to generate a multidimensional label-free profile of the TiME. The ubiquitous nature of label-free microscopy has helped utilize it to study a diverse range of TiMEs including cancer prognosis [114], neuronal dynamics [116], embryo development [117], and skeletal muscle development [118].

2.6. ELASTOGRAPHY

Elastography has emerged as a powerful technique for *in vivo*, non-invasive measurement of the mechanical properties in soft tissue microenvironments. Ultrasound elastography (USE) [119], magnetic resonance elastography (MRE) [120], optical coherence elastography (OCE) [121], and X-ray elastography [122] are some of the major categories of elastography based on different physical principles. Three general steps are involved in elastography measurements; tissue perturbation using static or dynamic forces; measuring the resulting deformations; and inferring the mechanical properties using appropriate models [123]. Fig. 3c describes the various methods for each approach. Different forms of elastography have been used clinically to evaluate a range of diseases including chronic liver fibrosis [124], breast [125] and brain tumours [126], multiple sclerosis [127], and skeletal muscle abnormalities [128], to name a few. Elastography has revolutionized the clinical diagnosis, monitoring, and treatment of many diseases that affect the TiME; MRE, for example, is currently the most accurate non-invasive approach for detecting and staging liver fibrosis. While remarkably successful, there are major limitations that restrict the utilization of this technique in more areas. For example, in USE, the shear waves attenuate rapidly as they penetrate the tissue, limiting the penetration depth and quality of the measurements *in vivo* [123]. Further, respiratory and cardiac motions, reverberations, and vessel pulsation could influence the US signal [129]. The elastography measurements are also highly dependent on the imaging protocol and skills of the operator [130]. Current techniques are focused on making the mechanism for mechanical deformation contact-free and localized, using photonic forces or ultrasound, that also help localize these forces for better mechanical resolution. Similarly, while assuming a mechanical model simplifies the problem of reconstructing the mechanical properties of the material, researchers have focused on building computational solutions, using Fourier-domain TiME difference or finite element modelling, for model-free characterization of tissues.

2.7. ATOMIC FORCE MICROSCOPY

Atomic force microscopy (AFM) is a unique tool for probing the TiME, with many applications in research and biomedicine since being introduced in 1986 [131] and has been increasingly used and improved since then. AFM can work in different modes of operation [132] to measure diverse properties at nano- and microscales, ranging from topography to mechanical properties. Elastic, viscoelastic, and poroelastic properties as well as high-resolution and non-destructive images of the surface can be acquired using this approach [133]. Put simply, during an AFM measurement, a probe interacts with the sample, scanning a small portion of the surface, with force and displacement of the probe being measured. AFM has allowed for the detailed analysis of cell-cell [134], cell-substrate

[135], and receptor-ligand interactions [136], as well as antibody aggregation [137], to name a few examples. AFM-based research has also led to several breakthroughs in drug development, delivery, and characterization [138]. Integrating AFM with optical microscopy, second-harmonic generation, scanning electron microscopy, and infrared spectroscopy has expanded the resolution and capabilities of these techniques [139,140]. Despite significant advances, several technical difficulties remain to be addressed. The TiME to image dynamic phenomenon, e.g., live-cell imaging, is often too long for adequate temporal resolution; movement of the TiME constituents reduces the spatial resolution of measurements; image acquisition is time-consuming and labour-intensive; and importantly, standardized protocols are needed to improve reproducibility [140].

2.8. ULTRASOUND MICROSCOPY

Perhaps due to its ubiquity in clinics everywhere, ultrasound imaging is often overlooked as a mechanical imaging modality even though the contrast in ultrasound imaging arises from the differences in the mechanical wave propagation through the sample. The spatial resolution of the typical clinical ultrasound imaging is too high due to using lower-frequency transducers (~10 MHz) that offer higher penetration depth, placing it beyond the scope of this paper. In 1987, Sherar et al. demonstrated one of the first B-scan ultrasound microscopes with a high-frequency 100-MHz transducer capable of 36- μm resolution in 3D [141], which was quickly applied to image tumour spheroids [141], skin [142], and the eye [143]. Besides the improvements to the transducer footprint and performance, there has been a focus on developing ultrasound contrasts over the years, specifically for imaging blood microvessels with diameters of less than 10 μm [144,145].

Despite being a critical component in physiology and the TiME, the dynamics of microvessels deep within tissues have remained inaccessible since imaging these fluid dynamics requires a technique with micron-scale spatial resolution, centimetre-scale penetration depth, and millisecond-scale speed [146]. Inspired by optical localization microscopy that enabled single-molecular imaging by selectively switching contrast agents on and off [147,148], ultrasound localization microscopy was developed using contrast agent microbubbles as ultrasound contrast agents whose scattering can be localized using ultrafast acquisition and spatiotemporal filtering [144,145] (Fig. 3c). In biomedical sciences, the development of ultrasound localization microscopy (ULM) enabled studying angiogenesis in cancer models in detail for theranostic applications [149], specifically in tracking the efficacy of anti-angiogenesis drugs longitudinally [150–152]. Similarly, imaging the microvasculature in the neuronal microenvironment elucidated aging-related changes such as a decrease in blood velocity, an increase in the vascular tortuosity, and the overall blood volume [153], and the process of neovascularization during and following neural injuries [154,155]. Current efforts in this field are targeted towards further improving spatial resolution without sacrificing the speed or penetration depth using deep-learning algorithms [156,157], which would enable translating ultrafast ULM to the clinical environment for versatile theranostic applications [158].

2.9. MULTIELECTRODE ARRAYS AND OPTICAL NEURAL PROBES

In 1963, Alan Hodgkin and Andrew Huxley won the Nobel Prize in Physiology for their contribution to understanding the mechanisms of action potentials in neurons using one of the first applications of voltage clamps [159,160]. Recording the electrical activity of cells at an intracellular, sub-cellular, or even within the local microenvironment has been historically achieved using invasive electrodes that must be inside, attached to, or close to the cells due to the low currents and high impedance [161]. Two avenues of advances, namely in microelectronics and optics, have made neurophysiology less invasive and more versatile. Engineering electrically conductive and biocompatible polymers that are flexible, stretchable, thin, and transparent have both enabled recordings from previously inaccessible tissue structures noninvasively and increased the data throughput of these measurements by increasing the density of electrodes within a small area [162–164]. Besides being used to study electrical activity patterns of organs such as the brain and the heart in animal models and humans, multielectrode arrays have also been used in high-throughput drug screening [164]. Since direct measurement of the electrical currents and potential requires some contact between the TiME and the probe, optical techniques offer a completely contactless alternative. Typically, optical probes are conjugated to ions that are activated upon sensing current flows or potential differences or to the ion channels to indicate activation (Fig. 3d). Combined with high-speed microscopy, optical probes have enabled neuroscience to move from relying on low-throughput electrophysiology to high-throughput optophysiology. Future work will focus on utilizing the high throughput of these techniques more effectively [165], increasing their versatility for clinical applications, and moving to label-free and less invasive probes.

2.10. HIGH-RESOLUTION MRI

Magnetic resonance imaging is a popular diagnostic technique that relies on the differences in the relaxation TiMEs of molecules under strong external magnetic fields for contrast. While typical MRI is restricted to cm-scale spatial resolution, using stronger external magnetic field strengths (~7T) and computational enhancements, MRI can achieve sub-mm resolution, generating highly detailed structural images of the human brain [166], prostate cancer [167], breast cancer [168], and the eye [169]. Functional MRI (fMRI), which measures the blood-oxygen-level-dependent (BOLD) contrast or blood-flow dynamics, has been used as an indirect measurement of neural activity as hemodynamics has been linked to neural activity in the brain since the 1990s [170]. High-resolution fMRI has been used to study the activity of specific brain regions in response to different stimuli [171,172]. This technique has not only been used as a diagnostic tool for neurological and neurodegenerative disorders [173,174] but also as a tool for fundamental studies in cognitive and behavioural neurosciences. fMRI is unique among the other sensing and imaging techniques discussed in this paper due to its high depth penetration and ability to measure whole organs within the body noninvasively. Some challenges to obtaining

high-resolution fMRI images have been its susceptibility to motion artifacts, high background due to baseline activity, long acquisition TiMEs for better spatiotemporal resolution, and difficulty in inferring the indirect relationship between the BOLD contrast and neural activity [175]. BOLD contrast in MRI has also been used in monitoring therapeutic effects in cancer [176,177]. Future research needs to address these challenges by maximizing the external field strength, enhancing the overall signals using contrast agents (such as thulium compounds and calcium indicators), and digital enhancement that sidesteps the need for long acquisition TiMEs.

This section presented an overview of our first pillar in the integrated approach. The techniques mentioned in this section span the vast spatial scales of TiME studies and have been successfully applied to evaluate the chemical, mechanical, and the electrical properties highlighted in Fig. 2. The recent technical advances and some highlighted applications discussed in this section are summarized in Table 1.

3. Modelling and fabricating time

The previous section described a multitude of methods to sense/probe structural, chemical, electrical, and mechanical dynamic properties of the TiME accurately and holistically. Yet, studies of TiME remain a daunting task due to the vast spatiotemporal scales involved. The techniques described in this section help simplify the TiME to enable specific and controlled studies. While several of these have existed for over a century, current focus is on scalability of these techniques, both in terms of the data generated and the overall complexity.

3.1. ARTIFICIAL PRODUCTION OF ECM COMPONENTS

Cells have historically been and continue to be traditionally cultured *in vitro* on 2D substrates [178–180]. However, cells or tissues cultured on 2D substrates (e.g., tissue culture plates or flasks) do not exhibit their *in vivo* physiology or growth characteristics and lack the expression of certain tissue-specific genes and proteins. Early studies that aimed to observe differences in cell structure and organization led to the understanding that the ECM in tissues not only provides structural support to tissues as initially thought but also interacts with cell surface receptors to initiate intracellular signals that promote gene expression for the maintenance of tissue homeostasis [181–184]. The ECM molecular complexes and their corresponding receptors on cells are differentially distributed among tissues and vary at different stages of development. There is incredible diversity among the different ECM constituents, ranging from

Table 1

Summary of the probing and sensing techniques for the multiscale physical, mechanical, chemical, and electrical characterization of the TiME.

Technique	Measurement/Mechanism	Recent technical advances	Biological and biomedical applications
FT-IR spectroscopy	Optical spectroscopy	Determination of secondary protein structures [7] Cellular ultrastructure with null-deflection IR spectroscopy [17] “Silent-region” tags [26–32]	Inflammatory bowel disease [11] Cancer histopathology [67] Predicting patient survival in cancer using FTIR measurements [6]
Quantitative phase imaging	Axial profiles of the samples and local refractive indices	Phase imaging with computational specificity [80] 3D phase imaging [86] Estimation of dry mass of cells [79]	Neuronal activity and disorders [83] Transmembrane proteins in cells [84]
Optical coherence tomography	Backscattering from refractive index mismatches detected through interferometry	Nanoparticles for enhanced scattering [48] Optical coherence elastography for mechanical properties [118] Blood oxygenation [91] Birefringence measurements [93]	Ophthalmic imaging [48,89] Cancer imaging [49]
Multiphoton label-free microscopy	Autofluorophores and harmonophores	Ultrashort tailored sources [69,107] Multimodal imaging [110–112] Fluorescence lifetime [108]	Metabolic imaging using optical redox ratios [96–98] Cancer prognosis [111] Neuronal dynamics [113] Embryo development [114]
Ultrasound imaging	Acoustic scattering from differences in density and elasticity	Ultrasound elastography for mechanical properties [116] Ultrasound super-resolution localization microscopy [144,145]	Liver biomechanics in fibrosis [121] Cancer biomechanics [122,127] Microangiography [150] Neurovascularization [151]
Multielectrode arrays	Microscale multiplexed measurements of electrical potentials and currents	Biocompatible stretchable and transparent polymers [159–161] Increasing the information throughput [162]	Electrical recordings from the brain and the heart [159–161] High-throughput drug screening [161]
Magnetic resonance imaging	Relaxation times of molecules under strong external magnetic fields	MR elastography for mechanical properties [123–125] Stronger external magnetic fields [163] Functional MRI [168–171]	Brain structure and activation [163, 170,172] Cancer therapeutics monitoring [173] High-resolution imaging of the eye [166]
Atomic force microscopy	Nanoindentation	Integration of AFM with optical microscopy, electron microscopy, and spectroscopy [17, 136,137]	Cell-cell and cell-substrate interactions [131–134] Antibody aggregation [134]

fibrillar collagens, elastin, and fibrins providing tensile strength, and glycosaminoglycans such as heparin and hyaluronic acid providing compressive strength, and adhesion proteins such as laminin and fibronectin to tether the ECM to the cellular components [185,186]. ECM proteins not only provide structural support but have profound effects on the cellular function and behaviour. Cell behaviours such as cell adhesion, migration, growth, differentiation, and apoptosis are known to be influenced by an ECM mechanism of signalling pathways from interactions between the ligand and corresponding receptor, typically integrins or proteoglycans [187]. A prime example is the interaction of fibronectin with surface integrins on a cell membrane to facilitate cellular transport. Upon interaction of the ECM with these receptors, the subunits in the cytoplasm initiate downstream signalling via the mitogen-activated protein kinase pathway [188]. This results in the activation/deactivation of genes that mediate cell migration. When growth factors and cytokine receptors are also involved in this interaction, there is a downstream expression of genes related to proliferation and differentiation, such as the focal adhesion kinase pathway [187]. Liver fibrosis is a typical example of such an interaction, where the increased concentrations of collagen and laminin causes defenestration of the liver sinusoidal endothelial cells and increased

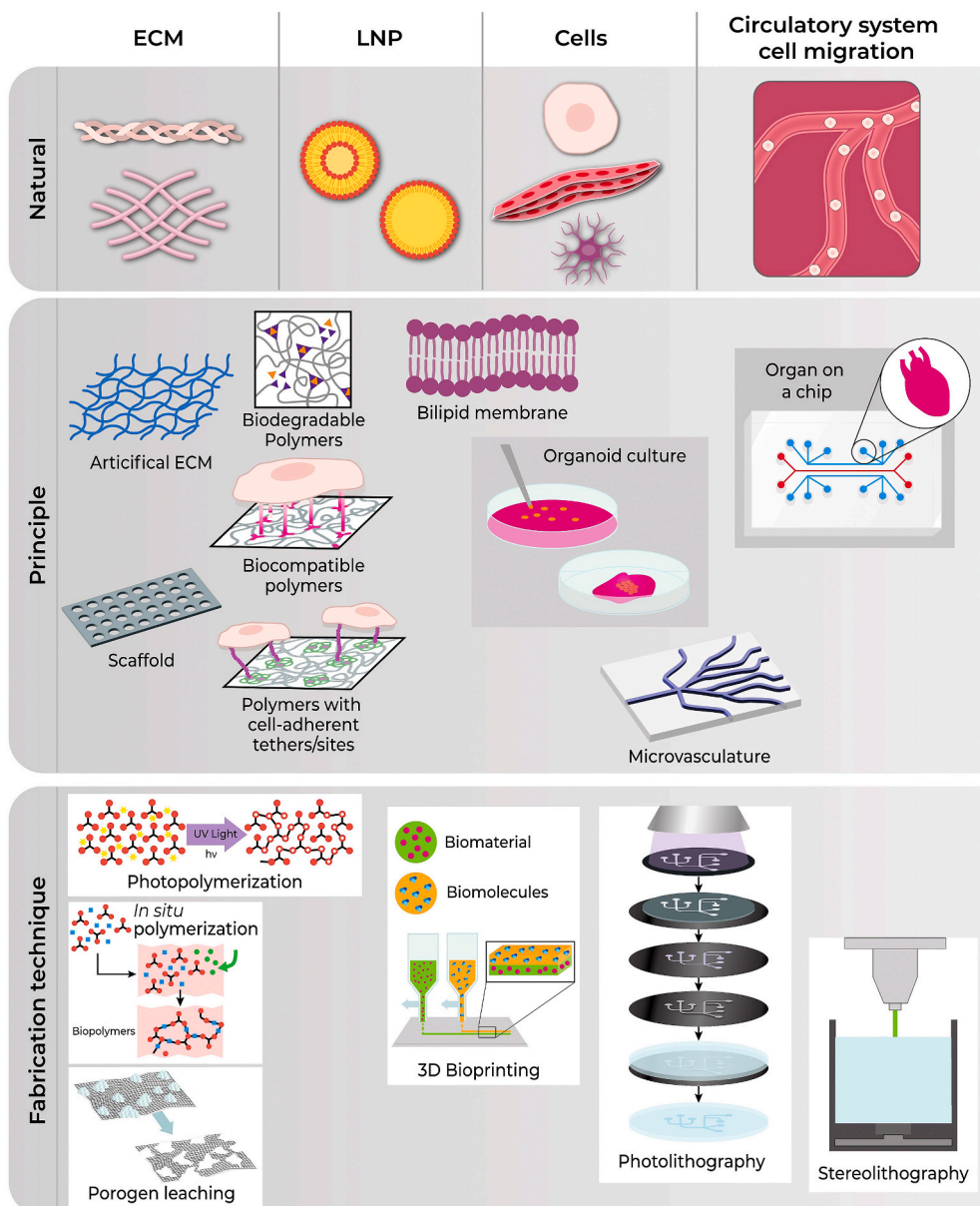


Fig. 4. Overview of the approach and example results of the techniques for modelling and fabricating TiME components categorized by the underlying engineering principles. The top row illustrates natural TiME components in ascending length scales from the left to right. The middle row illustrates artificial equivalents for the natural TiME components. The bottom row lists a few techniques used to fabricate the components in Row 2.

expression of the associated integrins that create a closed-loop excessive cellular proliferation and ECM generation [189]. On the other hand, lack of sufficient interactions between the receptors and the ECM matrix can lead to anoikis, which is the cell death mechanism triggered by lack of cell-attachment. Therefore, from a biological perspective, in any model of the TiME, the ECM must be designed carefully to both physically and chemically match the native functionalities.

From a tissue engineering perspective, being able to build a culture environment that can accurately mimic the native tissue is crucial for acquiring reproducible and relevant data. Making accurate models that include extracellular matrix, and can allow for soluble factors, is essential. The earliest artificial ECM components were naturally occurring polysaccharides like alginate [190] or agarose [184]. Advancements in polymer engineering and fabrication techniques have led to the development of artificial biocompatible polymer scaffolds for tissue cultures with silicone (polydimethylsiloxane) [191], ethylene (polyethylene glycol) [192], or lactic and glycolic acids (poly lactic-co-glycolic acid) [193] backbones. Hydrogels are three-dimensional, hydrophilic, polymeric networks with the ability to absorb water or biological fluids, and contain pores and soft consistency, similar to the natural tissue. Hydrogels have been fabricated using a great variety of natural and synthetic materials including collagen [194], hyaluronic acid [195], chondroitin sulphate [196], fibronectin [197], chitosan [198], and silk [199]. The material choice is based on the hydrophobicity of the required application, the degree of tunability of the matrix, and the anticipated interactions between the cellular components and the ECM [200]. These synthetic “designer” matrices have been shown to promote cellular functionalities like stem-cell mechanotransduction [201], neuronal growth and synapse formation [202], and chondrocyte production for cartilage tissue repair [203]. Recent hydrogel technologies have focused on the implementation of decellularized native tissue accompanied by the traditional and tissue relevant extracellular matrix components. Work by Danko et al., carefully characterized and developed a model using hydrogel as metastatic models for breast cancers *in vitro* [204]. End points such as metabolic phenotype and metabolic plasticity, and drug response were successfully characterized, showing that breast cancer that metastasizes to different tissues can potentially have other metabolic vulnerabilities that can be specifically targeted, and thereby provide more information for therapeutic intervention for patients with metastatic disease.

The use of hydrogels for biological applications first started in 1960 [205,206]. Since then, hydrogels have been the subject of extensive research, finding increasing applications in tissue engineering and drug delivery. The development of hydrogels can be divided into three phases; the first-generation hydrogels had high swelling and good mechanical strength (1960s); the second-generation hydrogels could respond to some stimuli such as changes in pH, specific biomolecules, and temperature (1970s) [207]; the third-generation hydrogels, including current ones, were composed of stereo complexed materials such as PEG-PLA and had tuneable, stimuli sensitive properties [208,209]. Nowadays, there are at least 30 FDA-approved injectable hydrogels on the market with a wide range of applications [210]; for example, hydrogels are being used for the protection of vulnerable tissue during cancer treatment, stimulation of natural collagen production, correction of facial wrinkles and folds, lumbar spinal fusion, treatment of female stress urinary incontinence, and treatment of advanced heart failure [210]. Some of the hydrogels have also been commercially very successful; Medtronic’s INFUSE, a collagen-based gel for bone regeneration, for example, has reached \$750 million in annual sales revenue [211]. Hydrogel-based systems hold exciting potential for helping even more patients in the coming years (Fig. 4).

3.2. ARTIFICIAL PRODUCTION OF CELLS AND SUB-CELLULAR STRUCTURES

Our understanding of the intricate processes within a cell continues to grow every day, in large part due to the advances in probing and sensing techniques described in the previous sections. One could argue that the natural step in the process is to recreate a cell from scratch, i.e., one that is self-enclosed, capable of generating its own energy through metabolism, survive in dynamic environments, and have the ability to grow and replicate [212]. This is a daunting goal that not only poses scientific challenges, but several ethical ones. However, fulfilling a part of these requirements is sufficient for most applications. The first criteria, i.e., a space self-enclosed by a lipid membrane was the first to be synthesized for artificial vesicles carrying a load, as capsosomes containing layer-by-layer liposomes, and as bi-phasic aqueous systems [213]. These simple sub-cellular compartments have also been combined in clever ways such as layering [214] or 3D bioprinting [215,216] to achieve cohesive units. Such units have been used to mimic cell-cell communication [217,218] and self-organization [219], as well as being used to modulate TiME as precise delivery agents. Over the years, the chemical information contained within could be specifically programmed, like DNA within cells, but on a much simpler basis. For instance, synthetic gene circuits, containing simple logical decisions based on cues from specific receptors and chemicals, were encoded within vesicles [220]. Initially developed as a bacterial toolbox (for *E. Coli*), these circuits have also been implemented in existing bulk systems to regulate cell functions [221]. Although division is a relatively simple task that could be achieved either in a bioreactor or even simple dilution based on the simplicity of the setup, replicating the metabolic process within these sub-systems is challenging considering that designing a metabolic mechanism capable of sustaining within a single unit has yet to be achieved. Although progress has been made in light-activated ATP cycles in liposomes using bacterial opsins [218], researchers have taken two approaches: either artificially creating a metabolic mechanism from bottom up or a top-down approach by using existing cells as models and stripping it to its basics [222, 223]. Current work has been focused on improving the adaptability and response of these components external factors by controlling the permeability of the membrane, increasing the complexity of the gene circuits, and in improving the biomimetic processes for specific organelles within the cells [224] (Fig. 4).

3.3. MICROFLUIDICS

Traditional methods of 3D culture in a static context can lead to accumulation of biochemical waste, accompanied by lack of nutrients and oxygen to the central portion of the organoid. This is counterproductive for a field that seeks to replicate physiologically

relevant dynamics. Microfluidic devices have been developed for the culture of spheroids to study applications such as regenerative medicine [225], vascularization [226], and drug targeting [227–229]. The commercially available DAX-1 microfluidics device developed by Aref et al., composes a central channel which can be mainly used to strategically place tumour cells, surrounded by two channels for media circulation [230]. These technologies have been used to characterize cellular interactions in the microenvironment including cancer cells and immune and stromal cells, for example, as well as the successful implementation of patient derived organotypic spheroids [231]. In addition, characterization of nutrient delivery, drug interaction through the vascular network have been demonstrated, as well as the emulation of tumour evolution driven by cell proliferation, angiogenesis, migration and intravasation. Overall, these systems are excellent tools for a dynamic integrated approach that recapitulates complex systems.

An interesting application of microfluidics in disease diagnostics is liquid biopsy. Liquid biopsies operate on the principles that biochemical environment of the bodily fluids, like urine, plasma, cerebrospinal fluids, and amniotic fluids, contain the markers of the disease states. This is not a novel concept in clinical diagnosis. For instance, estimation of the protein/enzyme levels in the blood form a core part of the diagnosis of certain metabolic and cardiovascular diseases. Infections in the brain are confirmed by lumbar punctures to draw cerebrospinal fluids. Liquid biopsies are relatively non-invasive. In a convergent approach, the liquid biopsies are processed efficiently in combination with the sensing techniques mentioned in the previous section for high-throughput screening of biomarkers by isolating cells, exosomes and extracellular vesicles, and free proteins and nucleic acids [232]. Recent advances in the screening for the rare circulating tumour cells in the blood include magnetically tagged high-throughput isolation [233] and label-free spiral sorting based on the haemodynamic forces [234]. Once isolated, advanced genomic screening can provide both disease-specific and patient-specific markers [235]. Similarly, the extracellular vesicles have been isolated from the liquid biopsies as potential early cancer biomarkers using label-free microscopy [236,237], droplet barcoding [238], and transcriptomics [239].

Recent advances in microfluidics have enabled unprecedented clinical applications that substantially improve patient care. The microfluidics market size is about \$23.6 billion [240] and is expected to grow even further in the coming years. Point-of-care (POC), miniaturized diagnostic systems, designed based on microfluidic principles, provide rapid test results for an increasing number of medical conditions [241]. The i-STAT system, for example, combines microfluidics and electrochemical analysis to analyse the blood chemistry in a handheld device [242]. The microfluidic and paper-based systems can isolate cancer cells, bacteria, biomolecules, and biomarkers to diagnose and monitor a wide range of diseases such as cancer, sickle cell disease, Zika, HIV, influenza, and sepsis [243]. Microfluidics has also been used for genome sequencing, and has contributed to a remarkable decrease in the cost and turnaround TIME of the test; rapid, low-cost sequencing has clinical significance, particularly for the diagnosis of rare diseases [244]. Microfluidics systems hold a great clinical potential to expand precision medicine; they can, for example, recapitulate many physical aspects of the tumour microenvironment and reveal the response of patient's cells to candidate drugs [245] (Fig. 4).

3.4. ELECTRICAL AND MAGNETIC FIELDS FOR TISSUE ENGINEERING

The effects of electric and magnetic stimulations in neurons, the electrically excitable cells in the body, have been well known and modelled since the 1950s [246]. Within a decade, the piezoelectric nature of the bone was discovered [247,248]; following which it was shown that the cellular differentiation in the bone could be affected by externally applied electrical currents [249,250]. Biological fibres like fibrin, collagen, and tubulin, and larger proteins such as amyloid beta respond to external electrical and magnetic fields because of their diamagnetic anisotropy and the anisotropy in their electrical polarizability [251]. These properties have been exploited to reorient the extracellular matrix to change its mechanical properties [252,253], to change the orientation, adhesion, and polarization of cells [254], and to modulate the fate of pluripotent cells [255,256], which have been applied to guide and accelerate wound healing [257,258]. Some major drawbacks of these studies are the weak susceptibility of natural fibres and proteins to external EM fields due to which the stimulation is preternaturally high and quite invasive.

As mentioned in Section 3.1, artificial ECMs have created a paradigm shift in tissue engineering and have been a driving force in their translation into the clinical environment. Making the ECMs more electromagnetically effectible would remove the need for invasive stimulation sources. On this note, two major trends have emerged in this field. For increasing the electrical susceptibility of artificial ECM, “smart” piezoelectric biomaterials have been developed, specifically for bone tissue engineering applications [259, 260]. Since delivering external magnetic fields are contactless and less invasive than electric fields, ferromagnetic materials have been incorporated into artificial ECMs [261,262] to noninvasively modulate the fate of stem cells in 3D biological models [263].

3.5. NEURAL PROSTHESIS

The neural prosthesis field involves the clinical use of tools developed based on principles of neurophysiology harnessing the fact that most physiological functions are coordinated and regulated by electrical signals. The ability to record and manipulate electrical signals in tissues was initially used to understand and characterize physiology. The field rapidly advanced to utilize electrical signal recording for diagnosis in clinical applications, and manipulation of electrical signals to attempt to mitigate pathology.

Implantable biosensors are valuable tools in neuroscience research and for clinical use as they provide direct recording of neurological signals and neurochemical processes. The need for devices that can be used for long-term studies has pushed the field towards advancing strategies to measure neurochemical levels through micro dialysis probes, which are diffusion-based devices to sample extracellular brain fluid, a widely used method to measure neurotransmitters in the neural tissue microenvironment. The field has further advanced to enable readouts of neurotransmitter levels *in vivo* using carbon fibre microelectrodes to oxidize or reduce electroactive species [264] and even multichannel sampling with enzymatic coatings to expand the detection range to neutrally charged electrochemicals [265]. A major limitation in the further development of these devices includes the brain tissue inflammatory

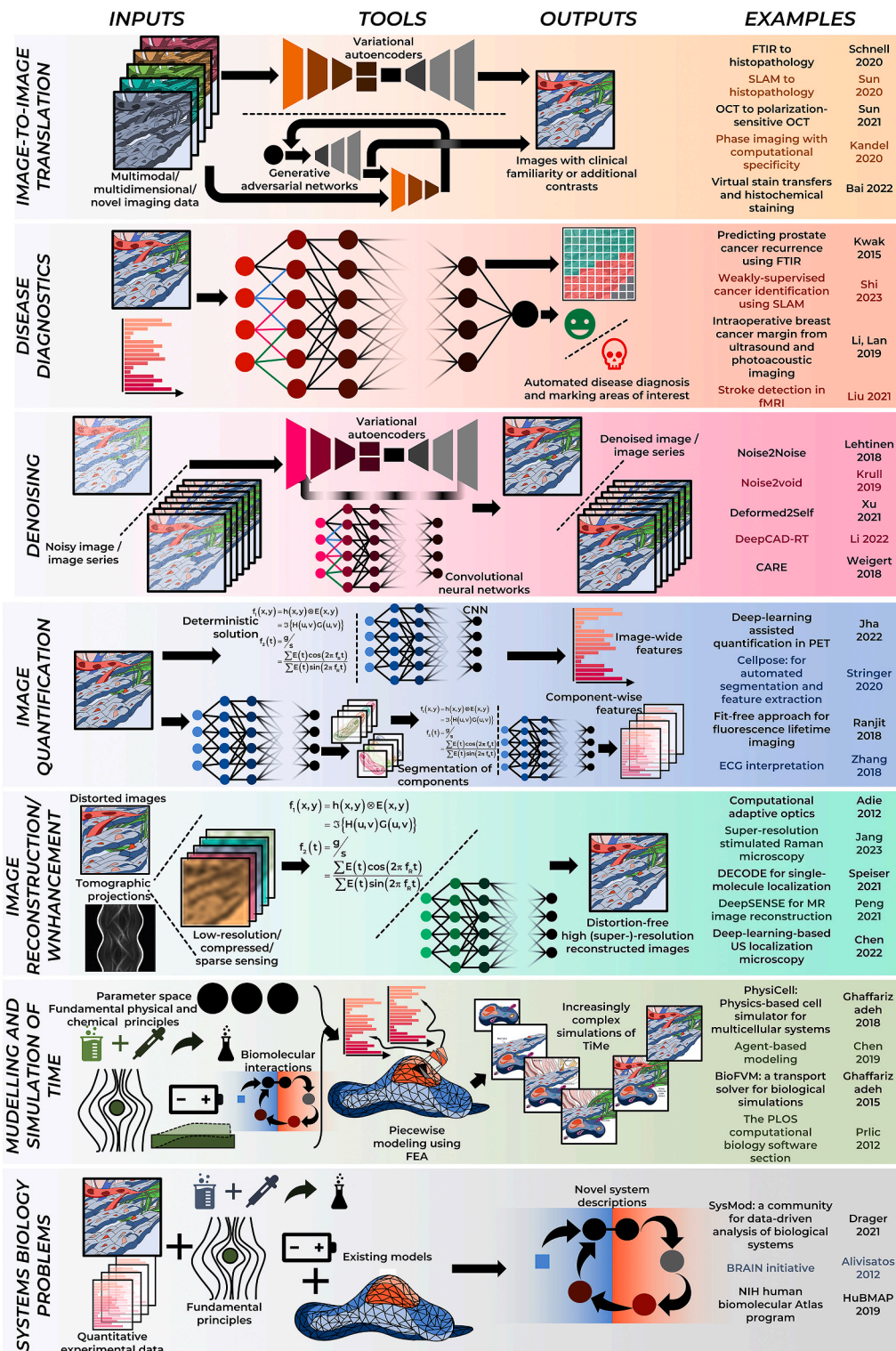


Fig. 5. The role of computational analysis in a convergent approach to studying TIME highlighting seven applications- (from the top) image-to-image translation [83,274–278], disease diagnostics [279–282], denoising [283–287], quantification [288–291], reconstruction and enhancement [292–296], simulation [297–300], and systems biology [301–303].

responses towards the devices, which alters the microenvironment being probed resulting in inaccurate signal measurements [266].

Among other successful clinical applications, spinal cord stimulators can be surgically implanted to induce selective and controlled electrical stimulation to control pain by exciting low-threshold mechanoreceptive afferents that excite the interneurons that inhibit projecting neurons that convey painful sensations through nociceptors [267]. Methods to guide the placement of electrical stimulation electrodes using buzzing sensations that patients can identify [268] enable modulation of appropriate cell microenvironments such as the dorsal root ganglia [269], which result in the most effective modulation. The development of neural prosthesis complements or in some cases even replaces pharmacologic approaches. In contrast to pharmacological approaches that are less effective as disease progresses, deep brain stimulation (DBS) provides improvements in motor symptoms in Parkinson's disease patients [270–272]. FDA-approved DBS-based therapies benefit patients that suffer complications from pharmacological platforms. DBS devices consist of implanting electrodes in specific anatomic sites capable of inducing neuromodulation to key neural tissue microenvironments and induce changes in cell function. DBS has proven safe and efficacious in multiple studies and presents the benefit of inducing minimal damage to the tissue microenvironment surrounding nerve cells compared to other invasive surgical interventions [273].

4. Computational analysis

From the 13th century description of rabbit population growth by Fibonacci in his eponymous sequence to Sir D'Arcy Thompson's 1917 book on recognizing the mathematical patterns in nature, scientists have sought to explain biological structures and processes using mathematical relationships. Consequently, biological systems have been described using simple principles, such as the Hodgkin-Huxley models for neurons and the cortical shell-liquid core model for suspended cells. In today's age of computing, the scope of computational analysis has expanded well beyond these simple descriptions. This rapid expansion can be attributed to three factors—increase in computing powers, growth of sensing and probing techniques that generate rich datasets, and development of artificial models of biological systems that enable high-throughput experimental studies.

Of course, the role of computing has been described in each niche of the tissue microenvironment with its own series of articles and reviews; simply reiterating them is beyond the scope of the paper. Also, algorithms largely arise independently of the application; thereby, requiring a separate structure if one wishes to study the intricacies of the algorithms. Furthermore, with rapidly burgeoning computing powers, most computing algorithms become obsolete within a few years. With large-scale collaborations, corporate investments, and accessible hardware and software resources, state-of-the-art algorithms are replaced by ones with vastly improved alternatives within months. Rather than tackling these issues, we instead describe the applications of computational analysis to bridge the sensing and modelling aspects of this convergent approach (Fig. 5).

4.1. COMPUTATIONAL TECHNIQUES FOR DATA ANALYSIS

As described in the previous sections, sensing and probing techniques continue to evolve to become multimodal and high throughput. Consequently, computational techniques are needed to utilize the information from these effectively. Over the last 20–30 years, for histopathology images alone, significant advancements have been made by using computer-aided and artificial intelligence-based techniques to study different TiME properties [304] from those digital images. Identification and segmentation of specific cellular or extra-cellular structures and counting the total number of cells are essential for diagnosing and grading different diseases [305,306]. Several image processing-based algorithms have been developed and studied for counting cells as a biomarker for disease, segmenting cells, nuclei, glands and so forth. In addition, several shape-based, radiometric, texture-based, chromatin-specific features extraction techniques have been studied to train machine learning-based classifiers for automated disease diagnosis. Recently, deep-learning-based methods have significantly outperformed the previously mentioned tasks [307,308]. State-of-the-art deep learning-based models like UNet, DeepLabV3, ResNet, InceptionV3 have been investigated to distinguish different TiME structures, to automatically classify different diseases. Very recently AI algorithms coupled with label-free imaging have been studied, this can add computational specificity to label-free microscopy images for different clinical tasks [308]. Traditionally, these methods need a large amount of labelled data for supervised training; this may not be readily available; hence semi-supervised or weakly supervised methods are currently being explored for performing these tasks [309,310] with lesser manual annotations.

The application of these advances has, of course, not been limited to just histopathology, but to every technique described in section 2. Broadly, we have classified the applications of computational analysis to sensing and probing into five categories: image-to-image translation, disease diagnostics, denoising, image quantification, and image enhancement. Among these, image quantification is perhaps the earliest application that has driven the progress of the others in the list. First, quantitative analysis of sensed data enables easy and effective repeatability of research. There have been several initiatives to tackle big problems cumulatively and collaboratively in biology; a key aspect to these is the standardization of datasets through quantification [311]. In its simplest implementation, quantitative sensing could be moving from arbitrary unit space to defined metrics. For instance, while fluorescent intensity is often measured as arbitrary units, fluorescence lifetime is a metric that is described in the ps-ns range, ensuring comparison across systems. Such a simple shift leads to several algorithms aiming to make tis estimation more accurate, faster, and more broadly applicable such as the real-time fitting [312], model-free approaches [289], or multiutility open source libraries [313]. In techniques where a direct quantification is not possible, deep-learning-based algorithms can enable interpretations of datasets that provide a quantitative basis for standardization, like echocardiogram (ECG) interpretation [291] or PET quantification [288]. Second, for broader utility, these algorithms have been packaged into readily useable and open-source libraries. Notable efforts towards this are CellProfiler [314] and Cellpose [290] packages that can extract thousands of biologically relevant features from biomedical datasets with minimal

supervision. Another task related to quantification is the need to study the individual components of the sensed datasets separately, which such packages also include.

Quantitative approaches to sensing enable creation of large datasets that can collated and analysed together. When applied in the context of disease diagnosis, models can be trained to discriminate between multiple disease states from multimodal sensed inputs. For instance, in micro spectroscopic techniques such as FTIR and Raman microscopy have been trained not only to segment the individual components but automatically estimate tumour margins for breast [315], prostate [2], and colon cancer applications. Similarly, multiphoton microscopy and ultrasound have been utilized intraoperatively for tumour margin assessment, even with minimal supervision [282] and for detection of ischemic stroke in real-time for MRI [281]. There are several hundred papers published each year about automated disease diagnosis using machine learning. A major limiting factor to the broader applicability of these in clinical applications is that a lot of these models are trained on homogenous and small datasets with no cross-modality translation potential. To solve this, large datasets must be built through needs high-throughput, fast, and high-quality techniques for sensing and probing.

A key factor that enables high-throughput sensing is the ability to transform sub-par datasets into high-quality ones through image enhancement and denoising. Denoising techniques often utilize the inherent redundancy in imaging techniques (such as video-rate or volumetric imaging) or contextual information from larger datasets to remove linear and nonlinear noise from these datasets [283–287]. The algorithms described in Fig. 5 are a small subset of those described in literature; new techniques continue to develop with broader applicability and better performance. Similarly, images are enhanced to have better resolution and information content using deep learning for fluorescence microscopy, ultrasound localization microscopy, and MRI. Even without deep learning, there are several deterministic approaches to correcting distortions and aberrations due to the imaging conditions, such as computational adaptive optics.

While these automated algorithms strive to minimize human inputs into disease diagnosis, an alternative approach is to present the rich dataset in familiar forms to the human for better decision making. For instance, clinical pathologists are often trained on histopathology slides. While techniques like FTIR and label-free multiphoton microscopy generate multimodal datasets faster and with less processing of these tissues, they may not be easily interpretable to these pathologists. Image-to-image translation approaches facilitate the broader applicability of these novel sensing techniques in the clinical environment today by converting these multidimensional images into synthetic histopathology images, which can then be annotated by pathologists [83,274–278]. These approaches have two additional advantages: the specificity of label-free techniques can be enhances using computational labelling (such as synthetic immunofluorescence datasets from quantitative phase images) and improving the cross-modality application of existing automated diagnosis algorithms.

4.2. COMPUTATIONAL MODELLING OF TiME FUNCTIONALITIES

Computational models of tissue microenvironments are essential to studying complex and dynamic relationships, mechanical and chemical communication between cells and extracellular matrix in a faster and more convenient way [316]. These computational models can be especially useful for cancer related studies where the simulation of oxygen transport and different growth factors may reveal valuable insights into the complex relationship between the microenvironment and cancer development. Different computational and mathematical cellular automata models have been developed to study growth and dynamical development, especially in the tumour microenvironment [317–319]. Specific computational models related to the interaction between cells and the ECM have been proposed and replicated the experimental finding in a much shorter time scale [320,321]. With the rapid development of accessible and powerful computing resources, more streamlined simulation tools are currently being made. These high-throughput studies hopefully will open a broader horizon to study and re-engineer different components of tissue and specific tumour microenvironments [322,323].

As 2D models of tissue or tumour microenvironment may not be sufficient to understand the dynamic communication among different components, especially when a tumour is present, it is important to develop 3D systems where the dynamic changes of biophysical and biochemical environments are present. As it is not always possible to study those systems experimentally, it is more convenient to develop a computer simulation platform to simulate microvascular flow, evolving biochemical and biomechanical environments of cells, ECM, and dynamic motion of tumour cell growth. In one of the very primary works, the evolution and physiology of glioma neurovasculature in 3D has been modelled using a lattice-free model [324]. Tang et al. [325] developed a dodecahedral model for epithelial cell morphogenesis. Despite the continuous success of these models, especially 3D tumour models, some issues still exist as the developed models are often naïve and over-simplistic. Hence, it is important to develop more sophisticated models that more accurately recapitulate the heterogeneity and physiological complexity.

The ultimate goal is to create comprehensive *in silico* representations of nature, which can be used to accurately predict arbitrary and unknown biological processes. This requires large scale collaborations, where experimental data is used to enhance existing models, which then drive the next experimental steps iteratively. The successes of the BRAIN initiative [326], human genome project [327], and the HuBMAP [303] continue to inspire several such large-scale efforts.

This section highlighted how computational analysis helps bridge the gap between sensing and bio fabrication. Because current efforts are largely focused on collating, combining, and interpreting the ginormous amounts of data available thus far, the emerging algorithms are largely “black box.” This has led to over-fitting problems and results biased by small datasets or anomalies. Concentrating on incorporating prior knowledge effectively into the deep learning models (such as physics-based deep learning) or building interpretable models can not only help with the previously described tasks but open new avenues for computational analysis in TiME studies, such as biomarker and drug discoveries, and complex Bio design strategies. The next section highlights two instances where the convergent approach to integrating the concepts in Sections 2-4 can drive biological and biomedical TiME discoveries.

5. Examples of convergent studies

5.1. ALL-OPTICAL SETUPS FOR DETERMINING NEURAL PATHWAYS FOR BEHAVIOUR

Studies of the neural microenvironment demand both non-invasive and high-throughput tools to observe the dynamics of the neural circuit effectively. While neural probes directly probe and measure electrical dynamics, their invasiveness limits the applications. Recent developments in optogenetics and optical microscopy techniques, described in the previous sections, have enabled the development of all-optical tools for electrophysiology [328,329]. We highlight three aspects of this research that are currently driving progress in this field.

The limited depth penetration due to absorption and scattering by the tissue restricts *in vivo* imaging in the visible wavelengths. Two strategies have enabled overcoming this issue by moving to longer wavelengths. First, the development of red-shifted voltage and calcium indicators has led to researchers using longer wavelengths for imaging neural responses, which have better penetration in tissues [330–334]. Second, utilizing the advances in ultrashort femtosecond near and mid-infrared beams for multiphoton absorption processes both for excitation and emission has extended imaging to the deeper regions of the brain [335–338]. These strategies have been employed both for head-mounted imaging using fibre-optic beam delivery [339,340] and intravital imaging after craniotomy [341] or through a transcranial window [338].

Multiphoton excitation of the optogenetics molecules also increases the precision of control [342]. Coherent control of excitable molecules is an increasingly popular strategy to evoke different responses in the same cell under similar excitation conditions by modulating the phase of the light in the spectral domain [343,344]. Similarly, red-shifted channelrhodopsin variants enable optical excitation deeper in the tissue due to lower absorption [345,346]. Recent studies have also shown the possibility of exciting the opsins at saturation with a narrow pulse at higher peak powers to evoke single action potentials from the desired neuron [347,348].

Holographic stimulation of multiple neurons simultaneously using spatial light modulators dramatically increases the throughput of these studies [347,349]. The rapid advances in digital holography technology in the last few years have enabled researchers to incorporate holographic stimulation of opsins into all the aforementioned tools. Studies that have utilized all-optical tools for electrophysiology have been able to map the neural network of the cerebral cortex in real time [350], and study the formation of 'memory' in the brain [351]. Future work in this field includes closed-loop approaches to controlling the neural circuit patterns [6], utilizing label-free strategies for excitation and imaging to improve the applicability of these studies, and applying these technologies for pathology, such as neurodegenerative disorders [352] (Fig. 1a).

5.2. HIGH-THROUGHPUT SCREENING FOR PERSONALIZED THERAPY FOR CANCER

A popular technique at the nexus of several techniques in the previous section at the brink of its translation between benchtop and bedside is high-throughput screening (HTS) [353]. Thousands to millions of biological compounds for a specific biological target can be examined for their ability to interact with biological or disease-related targets through HTS [354,355]. A typical workflow for HTS involves a tissue-mimicking artificial microenvironment, typically a microwell or a hydrogel, with the cellular components of interest embedded within. Several microwells or samples could be grown independently in a single unit. This is usually integrated with a microfluidic chamber for controlled introduction of external agents and factors such as labels, modulators, or therapeutics. Finally, the whole setup is made amenable to be observed with a non-invasive imaging technique for continuous monitoring. From biopharmaceuticals to personalized therapy, HTS provides a clear pathway to scale up TiME studies for practical applications.

For instance, in the pharmaceutical industry spent over 87 billion USD on research and development in 2019, over 90% of which could not be developed into end products [356]. Having early and rapid screening procedures could bring down these costs significantly. Among the biopharmaceutical industry, cells grown in 2D and 3D microwell plates are introduced to several variations of the same drug and continuously monitored with optical imaging for evaluating the performance of the drug [357,358]. The whole process can even be automated completely, avoiding human effort and errors [359]. Apart from 2D *in vitro* models, there has been an active effort to use organ-on-a-chip models to holistically evaluate the performance on the drug in different components of the tissue and fine tune the delivery mechanism simultaneously [360].

While the aim of HTS in drug discovery is to accurately predict the behaviour of a drug for a diverse set of samples, HTS in personalized therapy is much more focused on predicting the outcomes for a specific sample from a single source for exposures to diverse conditions, often employing an organoid model [361]. Human organoids, which replicate *in vivo* 3D properties of diverse human tissues or tumours, are more physiologically relevant than 2D culture to study disease phenotypes. 3D cancer organoids derived from patients' tumours have been increasingly investigated for their potential utility for personalized treatment, where an array of drug combinations can be tested for their efficacies on a particular tumour phenotype *in vitro* before administering these *in vivo* [362, 363]. Studies have shown that personalized therapy for cancer have not only improved treatment outcomes in both human and animal models, but also reduced adverse effects of chemotherapeutic drugs [364,365]. The use of organoids for HTS has remained challenging due to limited sample sizes from patient tumours (typically obtained during biopsy) and lack of repeatability among different setups. Cell-free approaches offer an effective solution for the scalability of these studies [366].

Multimodal imaging systems and multidimensional imaging not only improves the quantity of feedback from the setup, but also enables AI-assisted screening. Using artificial intelligence on these datasets can further scale up the throughput [367], uncovering thousands of features within seconds. Current efforts are focused on improving the reliability and repeatability of HTS datasets across different systems and improving the interpretability of the AI-generated outputs [368]. For personalized therapy, HTS and other sequencing techniques combined with multi-omics disease modelling (e.g., genomics, proteomics and so on) have enabled a paradigm

shift to precision medicine which can provide accurate and personalized treatment to patients by bridging the gap between research and medical treatment (Fig. 1b).

6. Summary comments and outlook

While the TiME has profound influences on development, function, and disease progression, it has proven to be exceptionally challenging to study due to the interconnected diversity spanning many length scales and properties bridging electrical, chemical, mechanical axes. Modern advances in three areas – sensing, computation, and fabrication – are enabling unprecedented opportunities for innovations that may allow harnessing our increased understanding of the TiME to benefit human health. As briefly reviewed in this manuscript, a number of analytical techniques have been developed to sample varied length scales and properties. While science continues to advance individual measurements towards a higher level of accuracy, precision, and speed, perhaps the most exciting aspect of these collective advances for TiME studies is the availability of multimodal data sets that record multiple properties in concert. Multimodal sets not only offer a comprehensive view of the TiME but also allow for correlations between properties and driving forces to be understood. Here, we provided an overview of some of the established and emerging techniques. Similarly, computing and fabrication techniques are increasing in sophistication and capability, offering unprecedented opportunities to model the TiME both physically and computationally. Combining advances in these three areas can not only allow observing both top-down and bottom-up models of the TiME but will permit an understanding of the TiME under various conditions and perturbations. These capabilities can allow for a visualization of “TiME in action,” the exploration of a large number of possible functional outcomes that are determined from the spatiotemporal complexity of the TiME.

To realize this vision for any specific situation, an integration of the various techniques and methods is needed. Even when it is not feasible or necessary to conduct a study with all these factors, being aware of these possibilities will allow the reader to focus on particular axes while being aware of others. Moreover, convergent thinking can inspire future advances. For example, new engineering approaches to fabrication that integrate sensing and ability to engender into a variety of model systems with different mechanical, biochemical or electrical capabilities can be evolved. The need for a convergent approach is essential to bring together these three pillars to address a specific scientific challenge related to the TiME. Engaging in a convergent approach is also timely with recent advances in the necessary disciplines, increased ability to communicate and synthesize with cyber resources and co-development of research infrastructure. The integration of knowledge, tools and approaches from the areas can be strongly coupled, allowing a co-development of complementary tools and techniques as well as modes of integrative thinking. Towards that end, involvement and education of the next generation of researchers is essential. A number of programs are supported by funding agencies to provide undergraduate and graduate students as well as postdoctoral fellows with such opportunities. In summary, a convergent approach to understanding the TiME is poised to become an important avenue for scientific advances that can benefit human health.

7. Data availability

No data was used for the research described in the article and is, therefore, not available at any public repository.

FUNDING

National Institute of Biomedical Imaging and Bioengineering (under National Institutes of Health, USA): T32EB019944.

Ethics declarations

Review and/or approval by an ethics committee was not needed for this study because no original experiments with animals or humans were performed in this research.

CRediT authorship contribution statement

Rishyashring R. Iyer: Writing – review & editing, Writing – original draft, Visualization, Data curation, Conceptualization. **Catherine C. Applegate:** Writing – original draft. **Opeyemi H. Arogundade:** Writing – original draft. **Sushant Bangru:** Writing – original draft. **Ian C. Berg:** Writing – original draft. **Bashar Emon:** Writing – original draft. **Marilyn Porrás-Gomez:** Writing – original draft. **Pei-Hsuan Hsieh:** Writing – original draft. **Yoon Jeong:** Writing – original draft. **Yongdeok Kim:** Writing – original draft. **Hailey J. Knox:** Writing – original draft. **Amir Ostadi Moghaddam:** Writing – original draft. **Carlos A. Renteria:** Writing – original draft. **Craig Richard:** Writing – original draft. **Ashlie Santaliz-Casiano:** Writing – original draft. **Sourya Sengupta:** Writing – original draft. **Jason Wang:** Writing – original draft. **Samantha G. Zambuto:** Writing – original draft. **Maria A. Zeballos:** Writing – original draft. **Marcia Pool:** Writing – review & editing, Supervision, Project administration, Conceptualization. **Rohit Bhargava:** Writing – review & editing, Supervision, Project administration, Funding acquisition, Conceptualization. **H. Rex Gaskins:** Writing – review & editing, Supervision, Project administration, Funding acquisition, Conceptualization.

Declaration of competing interest

The authors declare that they have no known competing financial interests or personal relationships that could have appeared to

influence the work reported in this paper.

Acknowledgements

This article was constructed as a part of the Tissue Microenvironment Training Program at the University of Illinois Urbana-Champaign, supported by a T32 grant from the National Institutes of Health and University of Illinois Urbana-Champaign (from the National Institute Of Biomedical Imaging And Bioengineering of the National Institutes of Health under Award Number T32EB019944). We would like to thank Dorothy R. Loudermilk for her help with the illustrations. We would like to acknowledge Profs. Stephen A. Boppart, John W. Erdman, Andrew Smith, Auinash Kalsotra, Gregory Underhill, Taher Saif, Rashid Bashir, Jefferson Chan, Thomas Gaj, Brendan Harley, Roy Dar, Hyunjoon Kong, Amy J. Wagoner Johnson, Joseph Irudayaraj, Zeynep Madak-Erdogan, and Mark Anastasio as the graduate advisors for the authors R.R.I – M.A.Z. We would like to thank Profs. Ioan Notingher, Stephen A. Boppart, Gabriel Popescu, Pengfei Song, Dirk Walther, Monica Fabiani, Gabriele Gratton, Bradley P. Sutton for providing the example results for the figures.

References

- [1] K. Kong, C.J. Rowlands, S. Varma, W. Perkins, I.H. Leach, A.A. Koloydenko, H.C. Williams, I. Notingher, Diagnosis of tumors during tissue-conserving surgery with integrated autofluorescence and Raman scattering microscopy, *Proc. Natl. Acad. Sci. U.S.A.* 110 (2013) 15189–15194, <https://doi.org/10.1073/pnas.1311289110>.
- [2] R. Bhargava, Towards a practical Fourier transform infrared chemical imaging protocol for cancer histopathology, *Anal. Bioanal. Chem.* 389 (2007) 1155–1169, <https://doi.org/10.1007/s00216-007-1511-9>.
- [3] Y. Park, C. Depersing, G. Popescu, Quantitative phase imaging in biomedicine, *Nature Photon* 12 (2018) 578–589, <https://doi.org/10.1038/s41566-018-0253-x>.
- [4] S. You, et al., Intravital imaging by simultaneous label-free autofluorescence-multiharmonic microscopy, *Nat. Commun.* 9 (2018) 2125, <https://doi.org/10.1038/s41467-018-04470-8>.
- [5] C. Huang, et al., Short acquisition time super-resolution ultrasound microvessel imaging via microbubble separation, *Sci. Rep.* 10 (2020) 6007, <https://doi.org/10.1038/s41598-020-62898-9>.
- [6] Y.-Z. Liu, et al., Simultaneous two-photon activation and imaging of neural activity based on spectral–temporal modulation of supercontinuum light, *Neurophoton* 7 (2020), <https://doi.org/10.1117/1.NPh.7.4.045007>.
- [7] L.T.K. Vo, et al., Predicting individuals' learning success from patterns of pre-learning MRI activity, *PLoS One* 6 (2011) e16093, <https://doi.org/10.1371/journal.pone.0016093>.
- [8] P. Lasch, J. Kneipp, *Biomedical Vibrational Spectroscopy*, Wiley-Interscience, Hoboken, N.J, 2010.
- [9] M.J. Baker, et al., Using Fourier transform IR spectroscopy to analyze biological materials, *Nat. Protoc.* 9 (2014) 1771–1791, <https://doi.org/10.1038/nprot.2014.110>.
- [10] I.W. Levin, R. Bhargava, Fourier transform infrared vibrational spectroscopic imaging: integrating microscopy and molecular recognition, *Annu. Rev. Phys. Chem.* 56 (2005) 429–474, <https://doi.org/10.1146/annurev.physchem.56.092503.141205>.
- [11] R. Bhargava, Digital histopathology by infrared spectroscopic imaging, *Annual Rev. Anal. Chem.* 16 (2023) 205–230, <https://doi.org/10.1146/annurev-anchem-101422-090956>.
- [12] D.C. Fernandez, R. Bhargava, S.M. Hewitt, I.W. Levin, Infrared spectroscopic imaging for histopathologic recognition, *Nat. Biotechnol.* 23 (2005) 469–474, <https://doi.org/10.1038/nbt1080>.
- [13] S. Tiwari, A. Kajdacsy-Balla, J. Whiteley, G. Cheng, K. Jirstrom, H. Birgisson, S.M. Hewitt, R. Bhargava, INFORM: INFRared-based ORganizational Measurements of tumor and its microenvironment to predict patient survival, *Sci. Adv.* 7 (2021) eabb8292, <https://doi.org/10.1126/sciadv.abb8292>.
- [14] H. Yang, S. Yang, J. Kong, A. Dong, S. Yu, Obtaining information about protein secondary structures in aqueous solution using Fourier transform IR spectroscopy, *Nat. Protoc.* 10 (2015) 382–396, <https://doi.org/10.1038/nprot.2015.024>.
- [15] V.A. Lorenz-Fonfria, Infrared difference spectroscopy of proteins: from bands to bonds, *Chem. Rev.* 120 (2020) 3466–3576, <https://doi.org/10.1021/acs.chemrev.9b00449>.
- [16] A. Sadat, I.J. Joye, Peak fitting applied to Fourier transform infrared and Raman spectroscopic analysis of proteins, *Appl. Sci.* 10 (2020) 5918, <https://doi.org/10.3390/app10175918>.
- [17] B.R. Wood, The importance of hydration and DNA conformation in interpreting infrared spectra of cells and tissues, *Chem. Soc. Rev.* 45 (2016) 1980–1998, <https://doi.org/10.1039/c5cs00511f>.
- [18] H. Ghimire, X. Hu, G. Qin, A.G. Unil Perera, Optimizing infrared spectral discrimination to enhance disease diagnostics: monitoring the signatures of inflammatory bowel diseases with anti-TNF α therapy, *Biomed. Opt. Express* 11 (2020) 4679–4694, <https://doi.org/10.1364/BOE.394895>.
- [19] M.R. Kole, R.K. Reddy, M.V. Schulmerich, M.K. Gelber, R. Bhargava, Discrete frequency infrared microspectroscopy and imaging with a tunable quantum cascade laser, *Anal. Chem.* 84 (2012) 10366–10372, <https://doi.org/10.1021/ac302513f>.
- [20] R. Bhargava, Infrared spectroscopic imaging: the next generation, *Appl. Spectrosc.* 66 (2012) 1091–1120, <https://doi.org/10.1366/12-06801>.
- [21] K. Yeh, et al., Infrared spectroscopic laser scanning confocal microscopy for whole-slide chemical imaging, *Nat. Commun.* 14 (2023) 5215, <https://doi.org/10.1038/s41467-023-40740-w>.
- [22] Y. Phal, L. Pfister, P.S. Carney, R. Bhargava, Resolution limit in infrared chemical imaging, *J. Phys. Chem. C* 126 (2022) 9777–9783, <https://doi.org/10.1021/acs.jpcc.2c00740>.
- [23] Q. Xia, J. Yin, Z. Guo, J.-X. Cheng, Mid-infrared photothermal microscopy: principle, instrumentation, and applications, *J. Phys. Chem. B* 126 (2022) 8597–8613, <https://doi.org/10.1021/acs.jpcc.2c05827>.
- [24] S. Kenkel, M. Gryka, L. Chen, M.P. Confer, A. Rao, S. Robinson, K.V. Prasanth, R. Bhargava, Chemical imaging of cellular ultrastructure by null-deflection infrared spectroscopic measurements, *Proc Natl Acad Sci U S A* 119 (2022) e2210516119, <https://doi.org/10.1073/pnas.2210516119>.
- [25] R.W. Hellwarth, Theory of stimulated Raman scattering, *Phys. Rev.* 130 (1963) 1850–1852, <https://doi.org/10.1103/PhysRev.130.1850>.
- [26] C.W. Freudiger, W. Min, B.G. Saar, S. Lu, G.R. Holtom, C. He, J.C. Tsai, J.X. Kang, X.S. Xie, Label-free biomedical imaging with high sensitivity by stimulated Raman scattering microscopy, *Science* 322 (2008) 1857–1861, <https://doi.org/10.1126/science.1165758>.
- [27] X.-S. Zheng, I.J. Jahn, K. Weber, D. Cialla-May, J. Popp, Label-free SERS in biological and biomedical applications: recent progress, current challenges and opportunities, *Spectrochim. Acta Mol. Biomol. Spectrosc.* 197 (2018) 56–77, <https://doi.org/10.1016/j.saa.2018.01.063>.
- [28] T. Vo-Dinh, SERS chemical sensors and biosensors: new tools for environmental and biological analysis, *Sensor. Actuator. B Chem.* 29 (1995) 183–189, [https://doi.org/10.1016/0925-4005\(95\)01681-3](https://doi.org/10.1016/0925-4005(95)01681-3).
- [29] C.L. Evans, E.O. Potma, M. Ptuoris'haag, D. Côté, C.P. Lin, X.S. Xie, Chemical imaging of tissue in vivo with video-rate coherent anti-Stokes Raman scattering microscopy, *Proc Natl Acad Sci U S A* 102 (2005) 16807–16812, <https://doi.org/10.1073/pnas.0508282102>.
- [30] J.-X. Cheng, Y.K. Jia, G. Zheng, X.S. Xie, Laser-scanning coherent anti-Stokes Raman scattering microscopy and applications to cell biology, *Biophys. J.* 83 (2002) 502–509, [https://doi.org/10.1016/S0006-3495\(02\)75186-2](https://doi.org/10.1016/S0006-3495(02)75186-2).

- [31] T.W. Kee, M.T. Cicerone, Simple approach to one-laser, broadband coherent anti-Stokes Raman scattering microscopy, *Opt. Lett.* 29 (2004) 2701, <https://doi.org/10.1364/OL.29.002701>.
- [32] T. Hellerer, A.M.K. Enejder, A. Zumbusch, Spectral focusing: high spectral resolution spectroscopy with broad-bandwidth laser pulses, *Appl. Phys. Lett.* 85 (2004) 25–27, <https://doi.org/10.1063/1.1768312>.
- [33] S. Egoshi, K. Dodo, M. Sodeoka, Deuterium Raman imaging for lipid analysis, *Curr. Opin. Chem. Biol.* 70 (2022) 102181, <https://doi.org/10.1016/j.cbpa.2022.102181>.
- [34] C.C. Horgan, et al., Molecular imaging of extracellular vesicles *in vitro* via Raman metabolic labelling, *J. Mater. Chem. B* 8 (2020) 4447–4459, <https://doi.org/10.1039/D0TB00620C>.
- [35] K.A. Okotrub, D.V. Shamaeva, N.V. Surovtsev, Raman spectra of deuterated hydrocarbons for labeling applications, *J. Raman Spectroscopy* 53 (2022) 297–309, <https://doi.org/10.1002/jrs.6279>.
- [36] B. Rudolf, A. Kubicka, M. Salmain, M. Palusiak, A.J. Rybarczyk-Pirek, S. Wojtulewski, Synthesis and characterization of new M(II) carbonyl complexes (M = Fe or Ru) including an η -1-N-maleimidato ligand. Reactivity studies with biological thiols, *J. Organomet. Chem.* 801 (2016) 101–110, <https://doi.org/10.1016/j.jorganchem.2015.10.027>.
- [37] S. Clède, F. Lambert, C. Sandt, Z. Gueroui, N. Delsuc, P. Dumas, A. Vessières, C. Policar, Synchrotron radiation FTIR detection of a metal-carbonyl tamoxifen analog. Correlation with luminescence microscopy to study its subcellular distribution, *Biotechnol. Adv.* 31 (2013) 393–395, <https://doi.org/10.1016/j.biotechadv.2012.01.023>.
- [38] L. Shi, et al., Mid-infrared metabolic imaging with vibrational probes, *Nat. Methods* 17 (2020) 844–851, <https://doi.org/10.1038/s41592-020-0883-z>.
- [39] J. Phelan, A. Altharawi, K.L.A. Chan, Tracking glycosylation in live cells using FTIR spectroscopy, *Talanta* 211 (2020) 120737, <https://doi.org/10.1016/j.talanta.2020.120737>.
- [40] L. Jauffred, A. Samadi, H. Klingberg, P.M. Bendix, L.B. Oddershede, Plasmonic heating of nanostructures, *Chem. Rev.* 119 (2019) 8087–8130, <https://doi.org/10.1021/acs.chemrev.8b00738>.
- [41] E. Petryayeva, U.J. Krull, Localized surface plasmon resonance: nanostructures, bioassays and biosensing—a review, *Anal. Chim. Acta* 706 (2011) 8–24, <https://doi.org/10.1016/j.aca.2011.08.020>.
- [42] P.K. Jain, Taking the heat off of plasmonic chemistry, *J. Phys. Chem. C* 123 (2019) 24347–24351, <https://doi.org/10.1021/acs.jpcc.9b08143>.
- [43] W.S. Yun, J.-H. Park, D.-K. Lim, C.-H. Ahn, I.-C. Sun, K. Kim, How did conventional nanoparticle-mediated photothermal therapy become “hot” in combination with cancer immunotherapy? *Cancers* 14 (2022) 2044, <https://doi.org/10.3390/cancers14082044>.
- [44] Y.B. Zheng, B. Kiraly, P.S. Weiss, T.J. Huang, Molecular plasmonics for biology and nanomedicine, *Nanomedicine* 7 (2012) 751–770, <https://doi.org/10.2217/nmm.12.30>.
- [45] A. Becker, C. Henssenius, K. Licha, B. Ebert, U. Sukowski, W. Semmler, B. Wiedenmann, C. Grötzinger, Receptor-targeted optical imaging of tumors with near-infrared fluorescent ligands, *Nat. Biotechnol.* 19 (2001) 327–331, <https://doi.org/10.1038/86707>.
- [46] K.M. Mayer, F. Hao, S. Lee, P. Nordlander, J.H. Hafner, A single molecule immunoassay by localized surface plasmon resonance, *Nanotechnology* 21 (2010) 255503, <https://doi.org/10.1088/0957-4484/21/25/255503>.
- [47] J.R. Lakowicz, Plasmonics in biology and plasmon-controlled fluorescence, *Plasmonics* 1 (2006) 5–33, <https://doi.org/10.1007/s11468-005-9002-3>.
- [48] R. Huschka, J. Zuloaga, M.W. Knight, L.V. Brown, P. Nordlander, N.J. Halas, Light-induced release of DNA from gold nanoparticles: nanoshells and nanorods, *J. Am. Chem. Soc.* 133 (2011) 12247–12255, <https://doi.org/10.1021/ja204578e>.
- [49] A. Wijaya, S.B. Schaffer, I.G. Pallares, K. Hamad-Schifferli, Selective release of multiple DNA oligonucleotides from gold nanorods, *ACS Nano* 3 (2009) 80–86, <https://doi.org/10.1021/nn800702n>.
- [50] W.-C. Law, K.-T. Yong, A. Baev, P.N. Prasad, Sensitivity improved surface plasmon resonance biosensor for cancer biomarker detection based on plasmonic enhancement, *ACS Nano* 5 (2011) 4858–4864, <https://doi.org/10.1021/nn2009485>.
- [51] A. Javeed, S. Qamar, S. Ali, M.A.T. Mustafa, A. Nusrat, S.K. Ghauri, Histological stains in the past, present, and future, *Cureus* (2021), <https://doi.org/10.7759/cureus.18486>.
- [52] M.W. Davidson, R.E. Campbell, Engineered fluorescent proteins: innovations and applications, *Nat. Methods* 6 (2009) 713–717, <https://doi.org/10.1038/nmeth1009-713>.
- [53] R.E. Bailey, A.M. Smith, S. Nie, Quantum dots in biology and medicine, *Phys. E Low-dimens. Syst. Nanostruct.* 25 (2004) 1–12, <https://doi.org/10.1016/j.physe.2004.07.013>.
- [54] M.M. Barroso, Quantum dots in cell biology, *J. Histochem. Cytochem.* 59 (2011) 237–251, <https://doi.org/10.1369/0022155411398487>.
- [55] F. Chen, P. Si, A. De La Zerda, J.V. Jokerst, D. Myung, Gold nanoparticles to enhance ophthalmic imaging, *Biomater. Sci.* 9 (2021) 367–390, <https://doi.org/10.1039/D0BM01063D>.
- [56] C.S. Kim, P. Wilder-Smith, Y.-C. Ahn, L.-H.L. Liaw, Z. Chen, Y.J. Kwon, Enhanced detection of early-stage oral cancer *in vivo* by optical coherence tomography using multimodal delivery of gold nanoparticles, *J. Biomed. Opt.* 14 (2009) 034008, <https://doi.org/10.1117/1.3130323>.
- [57] A. Burns, H. Ow, U. Wiesner, Fluorescent core-shell silica nanoparticles: towards “Lab on a Particle” architectures for nanobiotechnology, *Chem. Soc. Rev.* 35 (2006) 1028–1042, <https://doi.org/10.1039/B600562B>.
- [58] A. Burns, P. Sengupta, T. Zedayko, B. Baird, U. Wiesner, Core/shell fluorescent silica nanoparticles for chemical sensing: towards single-particle laboratories, *Small* 2 (2006) 723–726, <https://doi.org/10.1002/sml.200600017>.
- [59] M. Fujii, R. Fujii, M. Takada, H. Sugimoto, Silicon quantum dot supraparticles for fluorescence bioimaging, *ACS Appl. Nano Mater.* 3 (2020) 6099–6107, <https://doi.org/10.1021/acsanm.0c01295>.
- [60] S.-T. Yang, et al., Carbon dots as nontoxic and high-performance fluorescence imaging agents, *J. Phys. Chem. C* 113 (2009) 18110–18114, <https://doi.org/10.1021/jp9085969>.
- [61] P. Yu, X. Wen, Y.-R. Toh, J. Tang, Temperature-dependent fluorescence in carbon dots, *J. Phys. Chem. C* 116 (2012) 25552–25557, <https://doi.org/10.1021/jp307308z>.
- [62] C. Gao, Y. Wang, Z. Ye, Z. Lin, X. Ma, Q. He, Biomedical micro-/nanomotors: from overcoming biological barriers to *in vivo* imaging, *Adv. Mater.* 33 (2021) 2000512, <https://doi.org/10.1002/adma.202000512>.
- [63] B. Esteban-Fernández De Ávila, A. Martín, F. Soto, M.A. Lopez-Ramirez, S. Campuzano, G.M. Vázquez-Machado, W. Gao, L. Zhang, J. Wang, Single cell real-time miRNAs sensing based on nanomotors, *ACS Nano* 9 (2015) 6756–6764, <https://doi.org/10.1021/acs.nano.5b02807>.
- [64] S. Chapman, K.J. Oparka, A.G. Roberts, New tools for *in vivo* fluorescence tagging, *Curr. Opin. Plant Biol.* 8 (2005) 565–573, <https://doi.org/10.1016/j.pbi.2005.09.011>.
- [65] X. Jiao, Y. Li, J. Niu, X. Xie, X. Wang, B. Tang, Small-molecule fluorescent probes for imaging and detection of reactive oxygen, nitrogen, and sulfur species in biological systems, *Anal. Chem.* 90 (2018) 533–555, <https://doi.org/10.1021/acs.analchem.7b04234>.
- [66] J. Yin, L. Huang, L. Wu, J. Li, T.D. James, W. Lin, Small molecule based fluorescent chemosensors for imaging the microenvironment within specific cellular regions, *Chem. Soc. Rev.* 50 (2021) 12098–12150, <https://doi.org/10.1039/D1CS00645B>.
- [67] M.A. Acosta, P. Ymele-Leki, Y.V. Kostov, J.B. Leach, Fluorescent microparticles for sensing cell microenvironment oxygen levels within 3D scaffolds, *Biomaterials* 30 (2009) 3068–3074, <https://doi.org/10.1016/j.biomaterials.2009.02.021>.
- [68] H.-J. Cho, et al., Tumor microenvironment-responsive fluorogenic nanoprobe for ratiometric dual-channel imaging of lymph node metastasis, *Colloids Surf. B Biointerfaces* 179 (2019) 9–16, <https://doi.org/10.1016/j.colsurfb.2019.03.047>.
- [69] K. Turcheniuk, V.N. Mochalin, Biomedical applications of nanodiamond, *Nanotechnology* 28 (2017) 252001, <https://doi.org/10.1088/1361-6528/aa6ae4> (Review).
- [70] G. Kucsko, P.C. Maurer, N.Y. Yao, M. Kubo, H.J. Noh, P.K. Lo, H. Park, M.D. Lukin, Nanometre-scale thermometry in a living cell, *Nature* 500 (2013) 54–58, <https://doi.org/10.1038/nature12373>.

- [71] F. Xu, et al., Quantum-enhanced diamond molecular tension microscopy for quantifying cellular forces, *Sci. Adv.* 10 (2024) eadi5300, <https://doi.org/10.1126/sciadv.adi5300>.
- [72] F. Hu, M.R. Lamprecht, L. Wei, B. Morrison, W. Min, Bioorthogonal chemical imaging of metabolic activities in live mammalian hippocampal tissues with stimulated Raman scattering, *Sci. Rep.* 6 (2016) 39660, <https://doi.org/10.1038/srep39660>.
- [73] L. Wei, F. Hu, Z. Chen, Y. Shen, L. Zhang, W. Min, Live-cell bioorthogonal chemical imaging: stimulated Raman scattering microscopy of vibrational probes, *Acc. Chem. Res.* 49 (2016) 1494–1502, <https://doi.org/10.1021/acs.accounts.6b00210>.
- [74] J. Seo, Y. Sim, J. Kim, H. Kim, I. Cho, H. Nam, Y.-G. Yoon, J.-B. Chang, PICASSO allows ultra-multiplexed fluorescence imaging of spatially overlapping proteins without reference spectra measurements, *Nat. Commun.* 13 (2022) 2475, <https://doi.org/10.1038/s41467-022-30168-z>.
- [75] J. Schnitzbauer, M.T. Strauss, T. Schlichthaerle, F. Schueder, R. Jungmann, Super-resolution microscopy with DNA-PAINT, *Nat. Protoc.* 12 (2017) 1198–1228, <https://doi.org/10.1038/nprot.2017.024>.
- [76] R. Hooke, *Micrographia, or Some Physiological Descriptions of Minute Bodies Made by Magnifying Glasses, with Observations and Inquiries Thereupon*, Jo. Martyn, and Ja. Allestry, printers to the Royal Society, London, 2024.
- [77] F. Zernike, Phase contrast, *Z Tech Physik* 16 (1935).
- [78] E. Hecht, *Optics*, 5 ed., Pearson Education, Inc, Boston, 2017.
- [79] B. Kemper, Bally G. Von, Digital holographic microscopy for live cell applications and technical inspection, *Appl. Opt.* 47 (2008) A52, <https://doi.org/10.1364/AO.47.000A52>.
- [80] B. Kemper, et al., *Label-free Quantitative in Vitro Live Cell Imaging with Digital Holographic Microscopy*, Springer Berlin Heidelberg, Berlin, Heidelberg, 2019, https://doi.org/10.1007/11663_2019_6.
- [81] W. Drexler, J.G. Fujimoto (Eds.), *Optical Coherence Tomography: Technology and Applications*, Springer International Publishing, Cham, 2015, <https://doi.org/10.1007/978-3-319-06419-2>.
- [82] S. Aknoun, J. Savatier, P. Bon, F. Galland, L. Abdeladim, B. Wattellier, S. Monneret, Living cell dry mass measurement using quantitative phase imaging with quadrature lateral shearing interferometry: an accuracy and sensitivity discussion, *J. Biomed. Opt.* 20 (2015) 126009, <https://doi.org/10.1117/1.JBO.20.12.126009>.
- [83] M.E. Kandel, et al., Phase imaging with computational specificity (PICS) for measuring dry mass changes in sub-cellular compartments, *Nat. Commun.* 11 (2020) 6256, <https://doi.org/10.1038/s41467-020-20062-x>.
- [84] M. Shan, M.E. Kandel, G. Popescu, Refractive index variance of cells and tissues measured by quantitative phase imaging, *Opt Express* 25 (2017) 1573, <https://doi.org/10.1364/OE.25.001573>.
- [85] P. Müller, M. Schürmann, S. Girardo, G. Cojoc, J. Guck, Accurate evaluation of size and refractive index for spherical objects in quantitative phase imaging, *Opt Express* 26 (2018) 10729, <https://doi.org/10.1364/OE.26.010729>.
- [86] P. Marquet, C. Depeursinge, P.J. Magistretti, Review of quantitative phase-digital holographic microscopy: promising novel imaging technique to resolve neuronal network activity and identify cellular biomarkers of psychiatric disorders, *Neurophoton* 1 (2014) 020901, <https://doi.org/10.1117/1.NPh.1.2.020901>.
- [87] J. Linares, A. Cantereau, L. Froux, F. Becq, Quantitative phase imaging to study transmembrane water fluxes regulated by CFTR and AQP3 in living human airway epithelial CFBE cells and CHO cells, *PLoS One* 15 (2020) e0233439, <https://doi.org/10.1371/journal.pone.0233439>.
- [88] Z. Wang, L. Millet, M. Mir, H. Ding, S. Unarunotai, J. Rogers, M.U. Gillette, G. Popescu, Spatial light interference microscopy (SLIM), *Opt Express* 19 (2011) 1016, <https://doi.org/10.1364/OE.19.001016>.
- [89] T.H. Nguyen, M.E. Kandel, M. Rubessa, M.B. Wheeler, G. Popescu, Gradient light interference microscopy for 3D imaging of unlabeled specimens, *Nat. Commun.* 8 (2017) 210, <https://doi.org/10.1038/s41467-017-00190-7>.
- [90] J. Fujimoto, E. Swanson, The development, commercialization, and impact of optical coherence tomography, *Invest. Ophthalmol. Vis. Sci.* 57 (2016) OCT1, <https://doi.org/10.1167/iovs.16-19963>.
- [91] E. Swanson, Commercialization of OCT: some views on the past, present, and future, in: *Biomedical Optics 2016*, OSA, Fort Lauderdale, Florida, 2016, pp. JW1A–3, <https://doi.org/10.1364/CANR.2016.JW1A.3>.
- [92] D. Cabrera Fernández, H.M. Salinas, C.A. Puliafito, Automated detection of retinal layer structures on optical coherence tomography images, *Opt Express* 13 (2005) 10200, <https://doi.org/10.1364/OPEX.13.010200>.
- [93] J. Kim, W. Brown, J.R. Maher, H. Levinson, A. Wax, Functional optical coherence tomography: principles and progress, *Phys. Med. Biol.* 60 (2015) R211–R237, <https://doi.org/10.1088/0031-9155/60/10/R211>.
- [94] D.J. Faber, E.G. Mik, M.C.G. Aalders, T.G. Van Leeuwen, Toward assessment of blood oxygen saturation by spectroscopic optical coherence tomography, *Opt. Lett.* 30 (2005) 1015, <https://doi.org/10.1364/OL.30.001015>.
- [95] J.A. Mulligan, G.R. Untracht, S.N. Chandrasekaran, C.N. Brown, S.G. Adie, Emerging approaches for high-resolution imaging of tissue biomechanics with optical coherence elastography, *IEEE J. Select. Topics Quantum Electron* 22 (2016) 246–265, <https://doi.org/10.1109/JSTQE.2015.2481705>.
- [96] M.J. Everett, K. Schoenberger, B.W. Colston, L.B. Da Silva, Birefringence characterization of biological tissue by use of optical coherence tomography, *Opt. Lett.* 23 (1998) 228, <https://doi.org/10.1364/OL.23.000228>.
- [97] P. Tang, M.A. Kirby, N. Le, Y. Li, N. Zeinstra, G.N. Lu, C.E. Murry, Y. Zheng, R.K. Wang, Polarization sensitive optical coherence tomography with single input for imaging depth-resolved collagen organizations, *Light Sci. Appl.* 10 (2021) 237, <https://doi.org/10.1038/s41377-021-00679-3>.
- [98] R.W. Boyd, *Nonlinear Optics*, third ed., Academic Press, Amsterdam ; Boston, 2008.
- [99] S.A. Boppart, S. You, L. Li, J. Chen, H. Tu, Simultaneous label-free autofluorescence-multiharmonic microscopy and beyond, *APL Photonics* 4 (2019) 100901, <https://doi.org/10.1063/1.5098349>.
- [100] A.C. Croce, G. Bottiroli, Autofluorescence spectroscopy and imaging: a tool for biomedical research and diagnosis, *Eur. J. Histochem.* (2014), <https://doi.org/10.4081/ejh.2014.2461>.
- [101] T.S. Blacker, M.D.E. Sewell, G. Szabadkai, M.R. Duchon, Metabolic profiling of live cancer tissues using NAD(P)H fluorescence lifetime imaging, in: M. Haznadar (Ed.), *Cancer Metabolism*, Springer New York, New York, NY, 2019, pp. 365–387, https://doi.org/10.1007/978-1-4939-9027-6_19.
- [102] W. Denk, J.H. Strickler, W.W. Webb, Two-Photon laser scanning fluorescence microscopy, *Science* 248 (1990) 73–76, <https://doi.org/10.1126/science.2321027>.
- [103] S.W. Hell, Three-photon excitation in fluorescence microscopy, *J. Biomed. Opt.* 1 (1996) 71, <https://doi.org/10.1117/12.229062>.
- [104] Y. Hontani, F. Xia, C. Xu, Multicolor three-photon fluorescence imaging with single-wavelength excitation deep in mouse brain, *Sci. Adv.* 7 (2021) eabf3531, <https://doi.org/10.1126/sciadv.abf3531>.
- [105] Y. Guo, P.P. Ho, A. Tirskliunas, F. Liu, R.R. Alfano, Optical harmonic generation from animal tissues by the use of picosecond and femtosecond laser pulses, *Appl. Opt.* 35 (1996) 6810, <https://doi.org/10.1364/AO.35.006810>.
- [106] J.A. Squier, M. Müller, G.J. Brakenhoff, K.R. Wilson, Third harmonic generation microscopy, *Opt Express* 3 (1998) 315, <https://doi.org/10.1364/OE.3.000315>.
- [107] D. Yelin, Y. Silberberg, Laser scanning third-harmonic-generation microscopy in biology, *Opt Express* 5 (1999) 169, <https://doi.org/10.1364/OE.5.000169>.
- [108] S. You, Y. Sun, E.J. Chaney, Y. Zhao, J. Chen, S.A. Boppart, H. Tu, Slide-free virtual histochemistry (Part I): development via nonlinear optics, *Biomed. Opt. Express* 9 (2018) 5240, <https://doi.org/10.1364/BOE.9.005240>.
- [109] J.R. Lakowicz, H. Szmacinski, K. Nowaczyk, M.L. Johnson, Fluorescence lifetime imaging of free and protein-bound NADH, *Proc Natl Acad Sci U S A* 89 (1992) 1271–1275, <https://doi.org/10.1073/pnas.89.4.1271>.
- [110] H. Tu, et al., Stain-free histopathology by programmable supercontinuum pulses, *Nature Photon* 10 (2016) 534–540, <https://doi.org/10.1038/nphoton.2016.94>.
- [111] J.E. Sorrells, R.R. Iyer, L. Yang, E.M. Martin, G. Wang, H. Tu, M. Marjanovic, S.A. Boppart, Computational photon counting using multithreshold peak detection for fast fluorescence lifetime imaging microscopy, *ACS Photonics* 9 (2022) 2748–2755, <https://doi.org/10.1021/acsp Photonics.2c00505>.

- [112] J.E. Sorrells, R.R. Iyer, L. Yang, E.J. Chaney, M. Marjanovic, H. Tu, S.A. Boppart, Single-photon peak event detection (SPEED): a computational method for fast photon counting in fluorescence lifetime imaging microscopy, *Opt Express* 29 (2021) 37759, <https://doi.org/10.1364/OE.439675>.
- [113] R.R. Iyer, et al., Label-free metabolic and structural profiling of dynamic biological samples using multimodal optical microscopy with sensorless adaptive optics, *Sci. Rep.* 12 (2022) 3438, <https://doi.org/10.1038/s41598-022-06926-w>.
- [114] Y. Sun, et al., Intraoperative visualization of the tumor microenvironment and quantification of extracellular vesicles by label-free nonlinear imaging, *Sci. Adv.* 4 (2018) eaau5603, <https://doi.org/10.1126/sciadv.aau5603>.
- [115] J. Kang, U. Kang, H.S. Nam, W. Kim, H.J. Kim, R.H. Kim, J.W. Kim, H. Yoo, Label-free multimodal microscopy using a single light source and detector for biological imaging, *Opt. Lett.* 46 (2021) 892, <https://doi.org/10.1364/OL.415938>.
- [116] A.J. Bower, C. Renteria, J. Li, M. Marjanovic, R. Barkalifa, S.A. Boppart, High-speed label-free two-photon fluorescence microscopy of metabolic transients during neuronal activity, *Appl. Phys. Lett.* 118 (2021) 081104, <https://doi.org/10.1063/5.0031348>.
- [117] N. Olivier, et al., Cell lineage reconstruction of early zebrafish embryos using label-free nonlinear microscopy, *Science* 329 (2010) 967–971, <https://doi.org/10.1126/science.1189428>.
- [118] Q. Sun, Y. Li, S. He, C. Situ, Z. Wu, J.Y. Qu, Label-free multimodal nonlinear optical microscopy reveals fundamental insights of skeletal muscle development, *Biomed. Opt Express* 5 (2014) 158, <https://doi.org/10.1364/BOE.5.000158>.
- [119] R.M.S. Sigrist, J. Liao, A.E. Kaffas, M.C. Chammas, J.K. Willmann, Ultrasound elastography: review of techniques and clinical applications, *Theranostics* 7 (2017) 1303–1329, <https://doi.org/10.7150/thno.18650>.
- [120] Y.K. Mariappan, K.J. Glaser, R.L. Ehman, Magnetic resonance elastography: a review, *Clin. Anat.* 23 (2010) 497–511, <https://doi.org/10.1002/ca.21006>.
- [121] K.V. Larin, D.D. Sampson, Optical coherence elastography – OCT at work in tissue biomechanics [Invited], *Biomed. Opt Express* 8 (2017) 1172, <https://doi.org/10.1364/BOE.8.001172>.
- [122] A. Sarvazyan, J. Hall T, W. Urban M, M.R. Fatemi, S. Aglyamov, S. Garra B, An overview of elastography—an emerging branch of medical imaging, *CMIR* 7 (2011) 255–282, <https://doi.org/10.2174/157340511798038684>.
- [123] M.M. Doyley, K.J. Parker, Elastography, *Ultrasound Clinics* 9 (2014) 1–11, <https://doi.org/10.1016/j.cult.2013.09.006>.
- [124] L. Castera, X. Forns, A. Alberti, Non-invasive evaluation of liver fibrosis using transient elastography, *J. Hepatol.* 48 (2008) 835–847, <https://doi.org/10.1016/j.jhep.2008.02.008>.
- [125] J. Bercoff, S. Chaffai, M. Tanter, L. Sandrin, S. Catheline, M. Fink, J.L. Gennisson, M. Meunier, *In vivo* breast tumor detection using transient elastography, *Ultrasound Med. Biol.* 29 (2003) 1387–1396, [https://doi.org/10.1016/S0301-5629\(03\)00978-5](https://doi.org/10.1016/S0301-5629(03)00978-5).
- [126] L. Xu, Y. Lin, J.C. Han, Z.N. Xi, H. Shen, P.Y. Gao, Magnetic resonance elastography of brain tumors: preliminary results, *Acta Radiol* 48 (2007) 327–330, <https://doi.org/10.1080/02841850701199967>.
- [127] J. Wu, et al., MR-elastography reveals degradation of tissue integrity in multiple sclerosis, *Neuroimage* 49 (2010) 2520–2525, <https://doi.org/10.1016/j.neuroimage.2009.06.018>.
- [128] M.A. Dresner, G.H. Rose, P.J. Rossman, R. Muthupillai, A. Manduca, R.L. Ehman, Magnetic resonance elastography of skeletal muscle, *J. Magn. Reson. Imaging* 13 (2001) 269–276, [https://doi.org/10.1002/1522-2586\(200102\)13:2<269::AID-JMRI1039>3.0.CO;2-1](https://doi.org/10.1002/1522-2586(200102)13:2<269::AID-JMRI1039>3.0.CO;2-1).
- [129] M. Bruce, O. Kolokythas, G. Ferraioli, C. Filice, M. O'Donnell, Limitations and artifacts in shear-wave elastography of the liver, *Biomed. Eng. Lett.* 7 (2017) 81–89, <https://doi.org/10.1007/s13534-017-0028-1>.
- [130] N. Ciledag, H. Kaygusuz, B. Sahin, E. Aktas, F.G.B. Imamoglu, B.K. Aribas, The advantages and limitations of ultrasound elastography in diagnosis of thyroid carcinoma, in: H. Ahmadzadehfar (Ed.), *Thyroid Cancer - Advances in Diagnosis and Therapy*, InTech, 2016, <https://doi.org/10.5772/64407>.
- [131] G. Binnig, C.F. Quate, Ch Gerber, Atomic force microscope, *Phys. Rev. Lett.* 56 (1986) 930–933, <https://doi.org/10.1103/PhysRevLett.56.930>.
- [132] P. Eaton, P. West, Atomic Force Microscopy, Oxford University Press, 2010, <https://doi.org/10.1093/acprof:oso/9780199570454.001.0001>.
- [133] A. Alessandrini, P. Facci, AFM: a versatile tool in biophysics, *Meas. Sci. Technol.* 16 (2005) R65–R92, <https://doi.org/10.1088/0957-0233/16/6/R01>.
- [134] P.-H. Puech, K. Poole, D. Knebel, D.J. Muller, A new technical approach to quantify cell–cell adhesion forces by AFM, *Ultramicroscopy* 106 (2006) 637–644, <https://doi.org/10.1016/j.ultramic.2005.08.003>.
- [135] T.D. Nguyen, Y. Gu, Investigation of cell-substrate adhesion properties of living chondrocyte by measuring adhesive shear force and detachment using AFM and inverse FEA, *Sci. Rep.* 6 (2016) 38059, <https://doi.org/10.1038/srep38059>.
- [136] C. Zhu, M. Long, S.E. Chesla, P. Bongrand, Measuring receptor/ligand interaction at the single-bond level: experimental and interpretative issues, *Ann. Biomed. Eng.* 30 (2002) 305–314, <https://doi.org/10.1114/1.1467923>.
- [137] O. Ouerghi, A. Touhami, A. Othmane, H. Ben Ouada, C. Martelet, C. Fretigny, N. Jaffrezic-Renault, Investigating antibody–antigen binding with atomic force microscopy, *Sensor. Actuator. B Chem.* 84 (2002) 167–175, [https://doi.org/10.1016/S0925-4005\(02\)00020-5](https://doi.org/10.1016/S0925-4005(02)00020-5).
- [138] U. Mauer, T. Velnar, M. Gaberšček, O. Planinšek, M. Finšgar, Recent progressive use of atomic force microscopy in biomedical applications, *TrAC, Trends Anal. Chem.* 80 (2016) 96–111, <https://doi.org/10.1016/j.trac.2016.03.014>.
- [139] A. Dazzi, C.B. Prater, AFM-IR: technology and applications in nanoscale infrared spectroscopy and chemical imaging, *Chem. Rev.* 117 (2017) 5146–5173, <https://doi.org/10.1021/acs.chemrev.6b00448>.
- [140] A. Stylianou, T. Stylianopoulos, Atomic force microscopy probing of cancer cells and tumor microenvironment components, *BioNanoSci* 6 (2016) 33–46, <https://doi.org/10.1007/s12668-015-0187-4>.
- [141] M.D. Sherar, M.B. Noss, F.S. Foster, Ultrasound backscatter microscopy images the internal structure of living tumour spheroids, *Nature* 330 (1987) 493–495, <https://doi.org/10.1038/330493a0>.
- [142] F.S. Foster, G.R. Lockwood, L.K. Ryan, K.A. Harasiewicz, L. Berube, A.M. Rauth, Principles and applications of ultrasound backscatter microscopy, *IEEE Trans. Ultrason., Ferroelect., Freq. Contr.* 40 (1993) 608–617, <https://doi.org/10.1109/58.238115>.
- [143] M.D. Sherar, B.G. Starkoski, W.B. Taylor, F.S. Foster, A 100 MHz B-Scan ultrasound backscatter microscope, *Ultrason Imaging* 11 (1989) 95–105, <https://doi.org/10.1177/016173468901100202>.
- [144] O. Couture, V. Hingot, B. Heiles, P. Muleki-Seya, M. Tanter, Ultrasound localization microscopy and super-resolution: a state of the art, *IEEE Trans. Ultrason., Ferroelect., Freq. Contr.* 65 (2018) 1304–1320, <https://doi.org/10.1109/TUFFC.2018.2850811>.
- [145] C. Errico, J. Pierre, S. Pezet, Y. Desailly, Z. Lenkei, O. Couture, M. Tanter, Ultrafast ultrasound localization microscopy for deep super-resolution vascular imaging, *Nature* 527 (2015) 499–502, <https://doi.org/10.1038/nature16066>.
- [146] Y. Desailly, J. Pierre, O. Couture, M. Tanter, Resolution limits of ultrafast ultrasound localization microscopy, *Phys. Med. Biol.* 60 (2015) 8723–8740, <https://doi.org/10.1088/0031-9155/60/22/8723>.
- [147] M.J. Rust, M. Bates, X. Zhuang, Sub-diffraction-limit imaging by stochastic optical reconstruction microscopy (STORM), *Nat. Methods* 3 (2006) 793–796, <https://doi.org/10.1038/nmeth929>.
- [148] E. Betzig, G.H. Patterson, R. Sougrat, O.W. Lindwasser, S. Olenych, J.S. Bonifacio, M.W. Davidson, J. Lippincott-Schwartz, H.F. Hess, Imaging intracellular fluorescent proteins at nanometer resolution, *Science* 313 (2006) 1642–1645, <https://doi.org/10.1126/science.1127344>.
- [149] F. Lin, S.E. Shelton, D. Espindola, J.D. Rojas, G. Pinton, P.A. Dayton, 3-D ultrasound localization microscopy for identifying microvascular morphology features of tumor angiogenesis at a resolution beyond the diffraction limit of conventional ultrasound, *Theranostics* 7 (2017) 196–204, <https://doi.org/10.7150/thno.16899>.
- [150] M. Lowerison, W. Zhang, X. Chen, T. Fan, P. Song, Characterization of anti-angiogenic chemo-sensitization via longitudinal ultrasound localization microscopy in colorectal carcinoma tumor xenografts, *IEEE Trans. Biomed. Eng.* 69 (2022) 1449–1460, <https://doi.org/10.1109/TBME.2021.3119280>.
- [151] J.D. Rojas, et al., Ultrasound measurement of vascular density to evaluate response to anti-angiogenic therapy in renal cell carcinoma, *IEEE Trans. Biomed. Eng.* 66 (2019) 873–880, <https://doi.org/10.1109/TBME.2018.2860932>.
- [152] I.G. Newsome, P.A. Dayton, Visualization of microvascular angiogenesis using dual-frequency contrast-enhanced acoustic angiography: a review, *Ultrasound Med. Biol.* 46 (2020) 2625–2635, <https://doi.org/10.1016/j.ultrasmedbio.2020.06.009>.

- [153] M.R. Lowerison, N.V.C. Sekaran, W. Zhang, Z. Dong, X. Chen, D.A. Llano, P. Song, Aging-related cerebral microvascular changes visualized using ultrasound localization microscopy in the living mouse, *Sci. Rep.* 12 (2022) 619, <https://doi.org/10.1038/s41598-021-04712-8>.
- [154] C. Demeñé, J. Robin, A. Dizeux, B. Heiles, M. Pernot, M. Tanter, F. Perren, Transcranial ultrafast ultrasound localization microscopy of brain vasculature in patients, *Nat. Biomed. Eng.* 5 (2021) 219–228, <https://doi.org/10.1038/s41551-021-00697-x>.
- [155] B. Belliard, C. Ahmanna, E. Tiran, K. Kanté, T. Deffieux, M. Tanter, F. Nothias, S. Soares, S. Pezet, Ultrafast Doppler imaging and ultrasound localization microscopy reveal the complexity of vascular rearrangement in chronic spinal lesion, *Sci. Rep.* 12 (2022) 6574, <https://doi.org/10.1038/s41598-022-10250-8>.
- [156] R.J.G. Van Sloun, O. Solomon, M. Bruce, Z.Z. Khaing, H. Wijkstra, Y.C. Eldar, M. Mischi, Super-resolution ultrasound localization microscopy through deep learning, *IEEE Trans. Med. Imaging* 40 (2021) 829–839, <https://doi.org/10.1109/TMI.2020.3037790>.
- [157] K. Christensen-Jeffries, et al., Super-resolution ultrasound imaging, *Ultrasound Med. Biol.* 46 (2020) 865–891, <https://doi.org/10.1016/j.ultrasmedbio.2019.11.013>.
- [158] T. Deffieux, C. Demene, M. Pernot, M. Tanter, Functional ultrasound neuroimaging: a review of the preclinical and clinical state of the art, *Curr. Opin. Neurobiol.* 50 (2018) 128–135, <https://doi.org/10.1016/j.conb.2018.02.001>.
- [159] A.L. Hodgkin, A.F. Huxley, Resting and action potentials in single nerve fibres, *J. Physiol.* 104 (1945) 176–195, <https://doi.org/10.1113/jphysiol.1945.sp004114>.
- [160] A.L. Hodgkin, A.F. Huxley, Action potentials recorded from inside a nerve fibre, *Nature* 144 (1939) 710–711, <https://doi.org/10.1038/144710a0>.
- [161] A. Vázquez-Guardado, Y. Yang, A.J. Bandodkar, J.A. Rogers, Recent advances in neurotechnologies with broad potential for neuroscience research, *Nat. Neurosci.* 23 (2020) 1522–1536, <https://doi.org/10.1038/s41593-020-00739-8>.
- [162] K.D. Wise, Silicon microsystems for neuroscience and neural prostheses, *IEEE Eng. Med. Biol. Mag.* 24 (2005) 22–29, <https://doi.org/10.1109/MEEMB.2005.1511497>.
- [163] M. Dipalo, et al., Plasmonic meta-electrodes allow intracellular recordings at network level on high-density CMOS-multi-electrode arrays, *Nature Nanotech* 13 (2018) 965–971, <https://doi.org/10.1038/s41565-018-0222-z>.
- [164] S.-J. Cho, T.-S. Nam, D. Byun, S.-Y. Choi, M.-K. Kim, S. Kim, Zebrafish needle EMG: a new tool for high-throughput drug screens, *J. Neurophysiol.* 114 (2015) 2065–2070, <https://doi.org/10.1152/jn.00538.2015>.
- [165] L. Paninski, J. Cunningham, Neural data science: accelerating the experiment-analysis-theory cycle in large-scale neuroscience, *Curr. Opin. Neurobiol.* 50 (2018) 232–241, <https://doi.org/10.1016/j.conb.2018.04.007>.
- [166] B.L. Edlow, et al., 7 Tesla MRI of the ex vivo human brain at 100 micron resolution, *Sci. Data* 6 (2019) 244, <https://doi.org/10.1038/s41597-019-0254-8>.
- [167] E.K. Vos, et al., Image quality and cancer visibility of T2-weighted magnetic resonance imaging of the prostate at 7 tesla, *Eur. Radiol.* 24 (2014) 1950–1958, <https://doi.org/10.1007/s00330-014-3234-6>.
- [168] M.A. Korteweg, W.B. Veldhuis, F. Visser, P.R. Luijten, WPTH.M. Mali, P.J. Van Diest, M.A.A.J. Van Den Bosch, D.J. Klomp, Feasibility of 7 tesla breast magnetic resonance imaging determination of intrinsic sensitivity and high-resolution magnetic resonance imaging, diffusion-weighted imaging, and 1H-magnetic resonance spectroscopy of breast cancer patients receiving neoadjuvant therapy, *Invest. Radiol.* 46 (2011) 370–376, <https://doi.org/10.1097/RLI.0b013e31820d7f06>.
- [169] R.K. Glarin, B.N. Nguyen, J.O. Cleary, S.C. Kolbe, R.J. Ordidge, B.V. Bui, A.M. McKendrick, B.A. Moffat, MR-EYE: high-resolution MRI of the human eye and orbit at ultrahigh field (7T), *Magn. Reson. Imag. Clin. N. Am.* 29 (2021) 103–116, <https://doi.org/10.1016/j.mric.2020.09.004>.
- [170] S. Ogawa, T.M. Lee, A.R. Kay, D.W. Tank, Brain magnetic resonance imaging with contrast dependent on blood oxygenation, *Proc. Natl. Acad. Sci. U.S.A.* 87 (1990) 9868–9872, <https://doi.org/10.1073/pnas.87.24.9868>.
- [171] E. Margalit, K.W. Jamison, K.S. Weiner, L. Vizioli, R.-Y. Zhang, K.N. Kay, K. Grill-Spector, 2020 ultra-high-resolution fMRI of human ventral temporal cortex reveals differential representation of categories and domains, *J. Neurosci.* 40 (2020) 3008–3024, <https://doi.org/10.1523/JNEUROSCI.2106-19>.
- [172] A.L. Pinho, et al., Individual Brain Charting, a high-resolution fMRI dataset for cognitive mapping, *Sci. Data* 5 (2018) 180105, <https://doi.org/10.1038/sdata.2018.105>.
- [173] E. Düzel, et al., European ultrahigh-field imaging network for neurodegenerative diseases (EUFIND), *Alzheimer's Dementia: Diagnosis, Assessment & Disease Monitoring* 11 (2019) 538–549, <https://doi.org/10.1016/j.dadm.2019.04.010>.
- [174] A. Abdulkadir, O. Ronneberger, R. Christian Wolf, B. Pfiederer, C. Saft, S. Kloppel, Functional and structural MRI biomarkers to detect pre-clinical neurodegeneration, *CAR* 10 (2013) 125–134, <https://doi.org/10.2174/1567205011310020002>.
- [175] J. Goense, Y. Bohraus, N.K. Logothetis, fMRI at high spatial resolution: implications for BOLD-models, *Front. Comput. Neurosci.* 10 (2016), <https://doi.org/10.3389/fncom.2016.00066>.
- [176] S. Gross, A. Gilead, A. Scherz, M. Neeman, Y. Salomon, Monitoring photodynamic therapy of solid tumors online by BOLD-contrast MRI, *Nat Med* 9 (2003) 1327–1331, <https://doi.org/10.1038/nm940>.
- [177] L. Jiang, P.T. Weatherall, R.W. McColl, D. Tripathy, R.P. Mason, Blood oxygenation level-dependent (BOLD) contrast magnetic resonance imaging (MRI) for prediction of breast cancer chemotherapy response: a pilot study, *J. Magn. Reson. Imaging* 37 (2013) 1083–1092, <https://doi.org/10.1002/jmri.23891>.
- [178] Y. Ni, R. Chen, Extracellular recombinant protein production from *Escherichia coli*, *Biotechnol. Lett.* 31 (2009) 1661–1670, <https://doi.org/10.1007/s10529-009-0077-3>.
- [179] D. Porro, M. Sauer, P. Branduardi, D. Mattanovich, Recombinant protein production in yeasts, *Mol. Biotechnol.* 31 (2005) 245–259, <https://doi.org/10.1385/MB:31:3:245>.
- [180] X. Zhang, M.R. Reagan, D.L. Kaplan, Electrospun silk biomaterial scaffolds for regenerative medicine, *Adv. Drug Deliv. Rev.* 61 (2009) 988–1006, <https://doi.org/10.1016/j.addr.2009.07.005>.
- [181] R.O. Hynes, Integrins: versatility, modulation, and signaling in cell adhesion, *Cell* 69 (1992) 11–25, [https://doi.org/10.1016/0092-8674\(92\)90115-s](https://doi.org/10.1016/0092-8674(92)90115-s).
- [182] R.L. Juliano, S. Haskill, Signal transduction from the extracellular matrix, *J. Cell Biol.* 120 (1993) 577–585, <https://doi.org/10.1083/jcb.120.3.577>.
- [183] C.A. Buck, A.F. Horwitz, Cell surface receptors for extracellular matrix molecules, *Annu. Rev. Cell Biol.* 3 (1987) 179–205, <https://doi.org/10.1146/annurev.cb.03.110187.001143>.
- [184] J. Folkman, A. Moscona, Role of cell shape in growth control, *Nature* 273 (1978) 345–349, <https://doi.org/10.1038/273345a0>.
- [185] R.O. Hynes, A. Naba, Overview of the matrisome—an inventory of extracellular matrix constituents and functions, *Cold Spring Harbor Perspect. Biol.* 4 (2012), <https://doi.org/10.1101/cshperspect.a004903> a004903–a004903.
- [186] A.J. Putnam, D.J. Mooney, Tissue engineering using synthetic extracellular matrices, *Nat Med* 2 (1996) 824–826, <https://doi.org/10.1038/nm0796-824>.
- [187] M. Petreaca, M. Martins-Green, Chapter 9 - the dynamics of cell-ECM interactions, with implications for tissue engineering, in: R. Lanza, R. Langer, J. Vacanti (Eds.), *Principles of Tissue Engineering*, fourth ed., Academic Press, Boston, 2014, pp. 161–187, <https://doi.org/10.1016/B978-0-12-398358-9.00009-4>.
- [188] A. Naba, K.R. Clauser, S. Hoersch, H. Liu, S.A. Carr, R.O. Hynes, The matrisome: *in silico* definition and *in vivo* characterization by proteomics of normal and tumor extracellular matrices, *Mol. Cell. Proteomics* 11 (2012), <https://doi.org/10.1074/mcp.M111.014647>. M111.014647.
- [189] R.O. Hynes, The extracellular matrix: not just pretty fibrils, *Science* 326 (2009) 1216–1219, <https://doi.org/10.1126/science.1176009>.
- [190] F. Lim, A.M. Sun, Microencapsulated islets as bioartificial endocrine pancreas, *Science* 210 (1980) 908–910, <https://doi.org/10.1126/science.6776628>.
- [191] M.M. Stanton, J.M. Rankenber, B.-W. Park, W.G. McGimpsey, C. Malcuit, C.R. Lambert, Cell behavior on surface modified polydimethylsiloxane (PDMS), *Macromol. Biosci.* 14 (2014) 953–964, <https://doi.org/10.1002/mabi.201300504>.
- [192] N.A. Alcantar, E.S. Aydil, J.N. Israelachvili, Polyethylene glycol-coated biocompatible surfaces, *J. Biomed. Mater. Res.* 51 (2000) 343–351, [https://doi.org/10.1002/1097-4636\(20000905\)51:3<343::aid-jbm7>3.0.co;2-d](https://doi.org/10.1002/1097-4636(20000905)51:3<343::aid-jbm7>3.0.co;2-d).
- [193] P.X. Ma, J.W. Choi, Biodegradable polymer scaffolds with well-defined interconnected spherical pore network, *Tissue Eng.* 7 (2001) 23–33, <https://doi.org/10.1089/107632701300003269>.
- [194] C. Yang, P.J. Hillas, J.A. Báez, M. Nokelainen, J. Balan, J. Tang, R. Spiro, J.W. Polarek, The application of recombinant human collagen in tissue engineering, *BioDrugs* 18 (2004) 103–119, <https://doi.org/10.2165/00063030-200418020-00004>.
- [195] G.D. Prestwich, Engineering a clinically-useful matrix for cell therapy, *Organogenesis* 4 (2008) 42–47, <https://doi.org/10.4161/org.6152>.

- [196] S. Varghese, N.S. Hwang, A.C. Canver, P. Theprungsirikul, D.W. Lin, J. Elisseeff, Chondroitin sulfate based niches for chondrogenic differentiation of mesenchymal stem cells, *Matrix Biol.* 27 (2008) 12–21, <https://doi.org/10.1016/j.matbio.2007.07.002>.
- [197] S.K. Seidlits, C.T. Drinnan, R.R. Petersen, J.B. Shear, L.J. Suggs, C.E. Schmidt, Fibronectin-hyaluronic acid composite hydrogels for three-dimensional endothelial cell culture, *Acta Biomater.* 7 (2011) 2401–2409, <https://doi.org/10.1016/j.actbio.2011.03.024>.
- [198] F. Ahmadi, Z. Oveisi, S.M. Samani, Z. Amoozgar, Chitosan based hydrogels: characteristics and pharmaceutical applications, *Res Pharm Sci* 10 (2015) 1–16.
- [199] S.H. Kim, et al., 3D bioprinted silk fibroin hydrogels for tissue engineering, *Nat. Protoc.* 16 (2021) 5484–5532, <https://doi.org/10.1038/s41596-021-00622-1>.
- [200] A. Bandzerevicz, A. Gadomska-Gajadur, Into the tissues: extracellular matrix and its artificial substitutes: cell signalling mechanisms, *Cells* 11 (2002) 914, <https://doi.org/10.3390/cells11050914>.
- [201] Q. Sun, F. Pei, M. Zhang, B. Zhang, Y. Jin, Z. Zhao, Q. Wei, Curved nanofiber network induces cellular bridge formation to promote stem cell mechanotransduction, *Adv. Sci.* 10 (2023) 2204479, <https://doi.org/10.1002/adv.202204479>.
- [202] T.C. Holmes, S. de Lacalle, X. Su, G. Liu, A. Rich, S. Zhang, Extensive neurite outgrowth and active synapse formation on self-assembling peptide scaffolds, *Proc Natl Acad Sci U S A* 97 (2000) 6728–6733, <https://doi.org/10.1073/pnas.97.12.6728>.
- [203] J. Kisiday, M. Jin, B. Kurz, H. Hung, C. Semino, S. Zhang, A.J. Grodzinsky, Self-assembling peptide hydrogel fosters chondrocyte extracellular matrix production and cell division: implications for cartilage tissue repair, *Proc Natl Acad Sci U S A* 99 (2002) 9996–10001, <https://doi.org/10.1073/pnas.142309999>.
- [204] T. Dankó, et al., Characterisation of 3D bioprinted human breast cancer model for *in vitro* drug and metabolic targeting, *Int. J. Mol. Sci.* 23 (2022) 7444, <https://doi.org/10.3390/ijms23137444>.
- [205] O. Wichterle, D. Lim, Hydrophilic gels for biological use, *Nature* 185 (1960) 117–118, <https://doi.org/10.1038/185117a0>.
- [206] S.C. Lee, I.K. Kwon, K. Park, Hydrogels for delivery of bioactive agents: a historical perspective, *Adv. Drug Deliv. Rev.* 65 (2013) 17–20, <https://doi.org/10.1016/j.addr.2012.07.015>.
- [207] S.J. Buwalda, K.W.M. Boere, P.J. Dijkstra, J. Feijen, T. Vermonden, W.E. Hennink, Hydrogels in a historical perspective: from simple networks to smart materials, *J Control Release* 190 (2014) 254–273, <https://doi.org/10.1016/j.jconrel.2014.03.052>.
- [208] Lh Yahia, History and applications of hydrogels, *J. Biomed. Sci.* 4 (2015), <https://doi.org/10.4172/2254-609X.100013>.
- [209] O. Yom-Tov, L. Neufeld, D. Seliktar, H. Bianco-Peled, A novel design of injectable porous hydrogels with in situ pore formation, *Acta Biomater.* 10 (2014) 4236–4246, <https://doi.org/10.1016/j.actbio.2014.07.006>.
- [210] A. Mandal, J.R. Clegg, A.C. Anselmo, S. Mitragotri, Hydrogels in the clinic, *Bioeng Transl Med* 5 (2020), <https://doi.org/10.1002/btm2.10158>.
- [211] J. Li, D.J. Mooney, Designing hydrogels for controlled drug delivery, *Nat. Rev. Mater.* 1 (2016) 16071, <https://doi.org/10.1038/natrevmats.2016.71>.
- [212] T. Gánti, *The Principles of Life*, Oxford University Press, Oxford ; New York, 2003.
- [213] L. Schoonen, J.C.M. Van Hest, Compartmentalization approaches in soft matter science: from nanoreactor development to organelle mimics, *Adv. Mater.* 28 (2016) 1109–1128, <https://doi.org/10.1002/adma.201502389>.
- [214] T. Kikuchi, T. Shimizu, M. Wada, M. Yamato, T. Okano, Automatic fabrication of 3-dimensional tissues using cell sheet manipulator technique, *Biomaterials* 35 (2014) 2428–2435, <https://doi.org/10.1016/j.biomaterials.2013.12.014>.
- [215] G. Villar, A.D. Graham, H. Bayley, A tissue-like printed material, *Science* 340 (2013) 48–52, <https://doi.org/10.1126/science.1229495>.
- [216] C. Xu, W. Chai, Y. Huang, R.R. Markwald, Scaffold-free inkjet printing of three-dimensional zigzag cellular tubes, *Biotechnol. Bioeng.* 109 (2012) 3152–3160, <https://doi.org/10.1002/bit.24591>.
- [217] A.F. Mason, N.A. Yewdall, P.L.W. Welzen, J. Shao, M. Van Stevendaal, J.C.M. Van Hest, D.S. Williams, L.K.E.A. Abdelmohsen, Mimicking cellular compartmentalization in a hierarchical protocell through spontaneous spatial organization, *ACS Cent. Sci.* 5 (2019) 1360–1365, <https://doi.org/10.1021/acscentsci.9b00345>.
- [218] G. Wang, K. Castiglione, Light-driven biocatalysis in liposomes and polymersomes: where are we now? *Catalysts* 9 (2018) 12, <https://doi.org/10.3390/catal9010012>.
- [219] D.S. Williams, A.J. Patil, S. Mann, Spontaneous structuration in coacervate-based protocells by polyoxometalate-mediated membrane assembly, *Small* 10 (2014) 1830–1840, <https://doi.org/10.1002/sml.1201303654>.
- [220] V. Noireaux, A. Libchaber, A vesicle bioreactor as a step toward an artificial cell assembly, *Proc. Natl. Acad. Sci. U.S.A.* 101 (2004) 17669–17674, <https://doi.org/10.1073/pnas.0408236101>.
- [221] J. Garamella, R. Marshall, M. Rustad, V. Noireaux, The all *E. coli* TX-TL toolbox 2.0: a platform for cell-free synthetic biology, *ACS Synth. Biol.* 5 (2016) 344–355, <https://doi.org/10.1021/acssynbio.5b00296>.
- [222] B.C. Buddingh, J.C.M. Van Hest, Artificial cells: synthetic compartments with life-like functionality and adaptivity, *Acc. Chem. Res.* 50 (2017) 769–777, <https://doi.org/10.1021/acs.accounts.6b00512>.
- [223] M.A. Boyd, N.P. Kamat, Designing artificial cells towards a new generation of biosensors, *Trends Biotechnol.* 39 (2021) 927–939, <https://doi.org/10.1016/j.tibtech.2020.12.002>.
- [224] L. Otrin, N. Marušić, C. Bednarz, T. Vidaković-Koch, I. Lieberwirth, K. Landfester, K. Sundmacher, Toward artificial mitochondrion: mimicking oxidative phosphorylation in polymer and hybrid membranes, *Nano Lett.* 17 (2017) 6816–6821, <https://doi.org/10.1021/acs.nanolett.7b03093>.
- [225] A. Zuchowska, E. Jastrzebska, M. Chudy, A. Dybko, Z. Brzozka, Advanced 3D spheroid culture for evaluation of photodynamic therapy in microfluidic system, *Procedia Eng.* 168 (2016) 403–406, <https://doi.org/10.1016/j.proeng.2016.11.184>.
- [226] Y. Nashimoto, R. Okada, S. Hanada, Y. Arima, K. Nishiyama, T. Miura, R. Yokokawa, Vascularized cancer on a chip: the effect of perfusion on growth and drug delivery of tumor spheroid, *Biomaterials* 229 (2020) 119547, <https://doi.org/10.1016/j.biomaterials.2019.119547>.
- [227] E.K. Sackmann, A.L. Fulton, D.J. Beebe, The present and future role of microfluidics in biomedical research, *Nature* 507 (2014) 181–189, <https://doi.org/10.1038/nature13118>.
- [228] P. Sabhachandani, S. Sarkar, S. Mckenney, D. Ravi, A.M. Evens, T. Konry, Microfluidic assembly of hydrogel-based immunogenic tumor spheroids for evaluation of anticancer therapies and biomarker release, *J Control Release* 295 (2019) 21–30, <https://doi.org/10.1016/j.jconrel.2018.12.010>.
- [229] V.S. Shirure, Y. Bi, M.B. Curtis, A. Lezia, M.M. Goedegebuure, S.P. Goedegebuure, R. Aft, R.C. Fields, S.C. George, Tumor-on-a-chip platform to investigate progression and drug sensitivity in cell lines and patient-derived organoids, *Lab Chip* 18 (2018) 3687–3702, <https://doi.org/10.1039/c8lc00596f>.
- [230] A.R. Aref, et al., 3D microfluidic *ex vivo* culture of organotypic tumor spheroids to model immune checkpoint blockade, *Lab Chip* 18 (2018) 3129–3143, <https://doi.org/10.1039/c8lc00322j>.
- [231] H.K. Hong, N.H. Yun, Y.-L. Jeong, J. Park, J. Doh, W.Y. Lee, Y.B. Cho, Establishment of patient-derived organotypic tumor spheroid models for tumor microenvironment modeling, *Cancer Med.* 10 (2021) 5589–5598, <https://doi.org/10.1002/cam4.4114>.
- [232] Y. Belotti, C.T. Lim, Microfluidics for liquid biopsies: recent advances, current challenges, and future directions, *Anal. Chem.* 93 (2021) 4727–4738, <https://doi.org/10.1021/acs.analchem.1c00410>.
- [233] A. Mishra, et al., Ultrahigh-throughput magnetic sorting of large blood volumes for epitope-agnostic isolation of circulating tumor cells, *Proc. Natl. Acad. Sci. U.S.A.* 117 (2020) 16839–16847, <https://doi.org/10.1073/pnas.2006388117>.
- [234] M.E. Warkiani, B.L. Khoo, L. Wu, A.K.P. Tay, A.A.S. Bhagat, J. Han, C.T. Lim, Ultra-fast, label-free isolation of circulating tumor cells from blood using spiral microfluidics, *Nat. Protoc.* 11 (2016) 134–148, <https://doi.org/10.1038/nprot.2016.003>.
- [235] M.J.M. Magbanua, et al., Expanded genomic profiling of circulating tumor cells in metastatic breast cancer patients to assess biomarker status and biology over time (CALGB 40502 and CALGB 40503, Alliance), *Clin. Cancer Res.* 24 (2018) 1486–1499, <https://doi.org/10.1158/1078-0432.CCR-17-2312>.
- [236] J.E. Sorrells, et al., Label-free nonlinear optical signatures of extracellular vesicles in liquid and tissue biopsies of human breast cancer, *Sci. Rep.* 14 (2024) 5528, <https://doi.org/10.1038/s41598-024-55781-4>.
- [237] A.V. Borisov, O.A. Zakharova, A.A. Samarina, N.V. Yunusova, O.V. Cheremisina, Y.V. Kistenev, A criterion of colorectal cancer diagnosis using exosome fluorescence-lifetime imaging, *Diagnostics* 12 (2022) 1792, <https://doi.org/10.3390/diagnostics12081792>.

- [238] M. Banijamali, et al., Characterizing single extracellular vesicles by droplet barcode sequencing for protein analysis, *J of Extracellular Vesicle* 11 (2022) 12277, <https://doi.org/10.1002/jev.2.12277>.
- [239] D. Yu, Y. Li, M. Wang, J. Gu, W. Xu, H. Cai, X. Fang, X. Zhang, Exosomes as a new frontier of cancer liquid biopsy, *Mol. Cancer* 21 (2022) 56, <https://doi.org/10.1186/s12943-022-01509-9>.
- [240] Grand View Research, *Microfluidics Market Size, Share & Trends Analysis Report by Technology (Medical/healthcare, Non-medical), by Material (Silicon, Glass, Polymer, PDMS, Others), by Application, by Region and Segment Forecasts, vols. 2023 – 2030, 2021*, p. 150.
- [241] S.K. Sia, L.J. Kricka, Microfluidics and point-of-care testing, *Lab Chip* 8 (2008) 1982, <https://doi.org/10.1039/b817915h>.
- [242] L.R. Volpatti, A.K. Yetisen, Commercialization of microfluidic devices, *Trends Biotechnol.* 32 (2014) 347–350, <https://doi.org/10.1016/j.tibtech.2014.04.010>.
- [243] J.M. Campbell, J.B. Balhoff, G.M. Landwehr, S.M. Rahman, M. Vaithyanathan, A.T. Melvin, Microfluidic and paper-based devices for disease detection and diagnostic research, *Int. J. Mol. Sci.* 19 (2018) 2731, <https://doi.org/10.3390/ijms19092731>.
- [244] Y.-C.C. Hou, et al., Precision medicine integrating whole-genome sequencing, comprehensive metabolomics, and advanced imaging, *Proc. Natl. Acad. Sci. U.S.A.* 117 (2020) 3053–3062, <https://doi.org/10.1073/pnas.1909378117>.
- [245] R. Maurya, N. Gohil, G. Bhattacharjee, K. Khambhati, K.J. Alzahrani, S. Ramakrishna, D.-T. Chu, V. Singh, Advances in microfluidics devices and its applications in personalized medicines, in: *Progress in Molecular Biology and Translational Science*, Elsevier, 2022, pp. 191–201, <https://doi.org/10.1016/bs.pmbts.2021.07.012>.
- [246] A.L. Hodgkin, A.F. Huxley, A quantitative description of membrane current and its application to conduction and excitation in nerve, *J. Physiol.* 117 (1952) 500–544, <https://doi.org/10.1113/jphysiol.1952.sp004764>.
- [247] E. Fukada, I. Yasuda, On the piezoelectric effect of bone, *J. Phys. Soc. Jpn.* 12 (1957) 1158–1162, <https://doi.org/10.1143/JPSJ.12.1158>.
- [248] C.A.L. Bassett, R.O. Becker, Generation of electric potentials by bone in response to mechanical stress, *Science* 137 (1962) 1063–1064, <https://doi.org/10.1126/science.137.3535.1063>.
- [249] C.A.L. Bassett, R.J. Pawluk, R.O. Becker, Effects of electric currents on bone in vivo, *Nature* 204 (1964) 652–654, <https://doi.org/10.1038/204652a0>.
- [250] R.O. Becker, D.G. Murray, A method for producing cellular dedifferentiation by means of very small electrical currents*, *Transactions of the New York Academy of Sciences* 29 (1967) 606–615, <https://doi.org/10.1111/j.2164-0947.1967.tb02430.x>.
- [251] C.N.M. Ryan, M.N. Doulgeroglou, D.I. Zeugolis, Electric field stimulation for tissue engineering applications, *BMC biomed eng* 3 (2021) 1, <https://doi.org/10.1186/s42490-020-00046-0>.
- [252] A. Privat-Maldonado, C. Bengtson, J. Razzakov, E. Smits, A. Bogaerts, Modifying the tumour microenvironment: challenges and future perspectives for anticancer plasma treatments, *Cancers* 11 (2019) 1920, <https://doi.org/10.3390/cancers11121920>.
- [253] P. Wust, B. Kortüm, U. Strauss, J. Nadobny, S. Zschaeck, M. Beck, U. Stein, P. Ghadjar, Non-thermal effects of radiofrequency electromagnetic fields, *Sci. Rep.* 10 (2020) 13488, <https://doi.org/10.1038/s41598-020-69561-3>.
- [254] C. Chen, X. Bai, Y. Ding, I.-S. Lee, Electrical stimulation as a novel tool for regulating cell behavior in tissue engineering, *Biomater. Res.* 23 (2019) 25, <https://doi.org/10.1186/s40824-019-0176-8>.
- [255] C.L. Ross, The use of electric, magnetic, and electromagnetic field for directed cell migration and adhesion in regenerative medicine, *Biotechnol Progress* 33 (2017) 5–16, <https://doi.org/10.1002/btpr.2371>.
- [256] G. Thirivikraman, S.K. Boda, B. Basu, Unraveling the mechanistic effects of electric field stimulation towards directing stem cell fate and function: a tissue engineering perspective, *Biomaterials* 150 (2018) 60–86, <https://doi.org/10.1016/j.biomaterials.2017.10.003>.
- [257] L. Leppik, et al., Combining electrical stimulation and tissue engineering to treat large bone defects in a rat model, *Sci. Rep.* 8 (2018) 6307, <https://doi.org/10.1038/s41598-018-24892-0>.
- [258] T. Saliev, Z. Mustapova, G. Kulsharova, D. Bulanin, S. Mikhailovsky, Therapeutic potential of electromagnetic fields for tissue engineering and wound healing, *Cell Prolif.* 47 (2014) 485–493, <https://doi.org/10.1111/cpr.12142>.
- [259] J. Jacob, N. More, K. Kalia, G. Kapusetti, Piezoelectric smart biomaterials for bone and cartilage tissue engineering, *Inflamm Regen* 38 (2018) 2, <https://doi.org/10.1186/s41232-018-0059-8>.
- [260] A. Zaszczynska, P. Sajkiewicz, A. Grady, Piezoelectric scaffolds as smart materials for neural tissue engineering, *Polymers* 12 (2020) 161, <https://doi.org/10.3390/polym12010161>.
- [261] S. Farzaneh, S. Hosseinzadeh, R. Samanipour, S. Hatamie, J. Ranjbari, A. Khojasteh, Fabrication and characterization of cobalt ferrite magnetic hydrogel combined with static magnetic field as a potential bio-composite for bone tissue engineering, *J. Drug Deliv. Sci. Technol.* 64 (2021) 102525, <https://doi.org/10.1016/j.jddst.2021.102525>.
- [262] Z. Liu, J. Liu, X. Cui, X. Wang, L. Zhang, P. Tang, Recent advances on magnetic sensitive hydrogels in tissue engineering, *Front. Chem.* 8 (2020) 124, <https://doi.org/10.3389/fchem.2020.00124>.
- [263] A. Pardo, M. Gómez-Florit, S. Barbosa, P. Taboada, R.M.A. Domingues, M.E. Gomes, Magnetic nanocomposite hydrogels for tissue engineering: design concepts and remote actuation strategies to control cell fate, *ACS Nano* 15 (2021) 175–209, <https://doi.org/10.1021/acsnano.0c08253>.
- [264] T.D.Y. Kozai, A.S. Jaquins-Gerstl, A.L. Vazquez, A.C. Michael, X.T. Cui, Brain tissue responses to neural implants impact signal sensitivity and intervention strategies, *ACS Chem. Neurosci.* 6 (2015) 48–67, <https://doi.org/10.1021/cn500256e>.
- [265] C. Pan, H. Wei, Z. Han, F. Wu, L. Mao, Enzymatic electrochemical biosensors for in situ neurochemical measurement, *Curr. Opin. Electrochem.* 19 (2020) 162–167, <https://doi.org/10.1016/j.coelec.2019.12.008>.
- [266] R.R. Holson, R.A. Gazzara, B. Gough, Declines in stimulated striatal dopamine release over the first 32 h following microdialysis probe insertion: generalization across releasing mechanisms, *Brain Res.* 808 (1998) 182–189, [https://doi.org/10.1016/S0006-8993\(98\)00816-6](https://doi.org/10.1016/S0006-8993(98)00816-6).
- [267] G.E. Loeb, Neural prosthetics: A review of empirical vs. Systems engineering strategies, *Applied Bionics and Biomechanics* 2018 (2018) 1–17, <https://doi.org/10.1155/2018/1435030>.
- [268] J. Holsheimer, Computer modelling of spinal cord stimulation and its contribution to therapeutic efficacy, *Spinal Cord* 36 (1998) 531–540, <https://doi.org/10.1038/sj.sc.3100717>.
- [269] J.-P. Van Buyten, I. Smet, L. Liem, M. Russo, F. Huygen, Stimulation of dorsal root ganglia for the management of complex regional pain syndrome: a prospective case series, *Pain Pract.* 15 (2015) 208–216, <https://doi.org/10.1111/papr.12170>.
- [270] E. Hogg, J. Wertheimer, S. Graner, M. Tagliati, Deep brain stimulation and nonmotor symptoms, in: *International Review of Neurobiology*, Elsevier, 2017, pp. 1045–1089, <https://doi.org/10.1016/bs.irn.2017.05.022>.
- [271] F.M. Weaver, Bilateral deep brain stimulation vs best medical therapy for patients with advanced Parkinson DiseaseA randomized controlled trial, *JAMA* 301 (2009) 63, <https://doi.org/10.1001/jama.2008.929>.
- [272] A. Williams, et al., Deep brain stimulation plus best medical therapy versus best medical therapy alone for advanced Parkinson’s disease (PD SURG trial): a randomised, open-label trial, *Lancet Neurol.* 9 (2010) 581–591, [https://doi.org/10.1016/S1474-4422\(10\)70093-4](https://doi.org/10.1016/S1474-4422(10)70093-4).
- [273] J.Y. Fang, C. Tolleson, The role of deep brain stimulation in Parkinson’s disease: an overview and update on new developments, *NDT* 13 (2017) 723–732, <https://doi.org/10.2147/NDT.S113998>.
- [274] B. Bai, et al., Label-free virtual HER2 immunohistochemical staining of breast tissue using deep learning, *BME Front* (2022), <https://doi.org/10.34133/2022/9786242>.
- [275] M. Schnell, S. Mittal, K. Falahkheirkhah, A. Mittal, K. Yeh, S. Kenkel, A. Kajdacsy-Balla, P.S. Carney, R. Bhargava, All-digital histopathology by infrared-optical hybrid microscopy, *Proc Natl Acad Sci U S A* 117 (2020) 3388–3396, <https://doi.org/10.1073/pnas.1912400117>.
- [276] Y. Sun, et al., Real-time three-dimensional histology-like imaging by label-free nonlinear optical microscopy, *Quant Imaging Med Surg* 10 (2020) 2177–2190, <https://doi.org/10.21037/qims-20-381>.
- [277] Y. Sun, J. Wang, J. Shi, S.A. Boppart, Synthetic polarization-sensitive optical coherence tomography by deep learning, *npj Digit. Med.* 4 (2021) 105, <https://doi.org/10.1038/s41746-021-00475-8>.

- [278] X. Yang, B. Bai, Y. Zhang, Y. Li, K. De Haan, T. Liu, A. Ozcan, Virtual stain transfer in histology via cascaded deep neural networks, *ACS Photonics* 9 (2022) 3134–3143, <https://doi.org/10.1021/acsp Photonics.2c00932>.
- [279] J.T. Kwak, A. Kajdacsy-Balla, V. Macias, M. Walsh, S. Sinha, R. Bhargava, Improving prediction of prostate cancer recurrence using chemical imaging, *Sci. Rep.* 5 (2015) 8758, <https://doi.org/10.1038/srep08758>.
- [280] R. Li, et al., High-speed intraoperative assessment of breast tumor margins by multimodal ultrasound and photoacoustic tomography, *Med Devices Sens* 1 (2018) e10018, <https://doi.org/10.1002/mds3.10018>.
- [281] C.-F. Liu, et al., Deep learning-based detection and segmentation of diffusion abnormalities in acute ischemic stroke, *Commun. Med.* 1 (2021) 61, <https://doi.org/10.1038/s43856-021-00062-8>.
- [282] J. Shi, H. Tu, J. Park, M. Marjanovic, A.M. Higham, N.N. Luckey, K.A. Craddock, Z.G. Liu, S.A. Boppart, Weakly supervised identification of microscopic human breast cancer-related optical signatures from normal-appearing breast tissue, *Biomed. Opt Express* 14 (2023) 1339–1354, <https://doi.org/10.1364/BOE.480687>.
- [283] A. Krull, T.-O. Buchholz, F. Jug, Noise2Void - Learning Denoising from Single Noisy Images, 2018, <https://doi.org/10.48550/ARXIV.1811.10980>.
- [284] J. Lehtinen, J. Munkberg, J. Hasselgren, S. Laine, T. Karras, M. Aittala, T. Aila, Noise2Noise: Learning Image Restoration without Clean Data, 2018, <https://doi.org/10.48550/ARXIV.1803.04189>.
- [285] X. Li, et al., Real-time denoising enables high-sensitivity fluorescence time-lapse imaging beyond the shot-noise limit, *Nat. Biotechnol.* 41 (2023) 282–292, <https://doi.org/10.1038/s41587-022-01450-8>.
- [286] M. Weigert, et al., Content-aware image restoration: pushing the limits of fluorescence microscopy, *Nat. Methods* 15 (2018) 1090–1097, <https://doi.org/10.1038/s41592-018-0216-7>.
- [287] J. Xu, E. Adalsteinsson, Deformed2Self: Self-Supervised Denoising for Dynamic Medical Imaging, 2021, <https://doi.org/10.48550/ARXIV.2106.12175>.
- [288] A.K. Jha, et al., Nuclear medicine and artificial intelligence: best practices for evaluation (the RELAINCE guidelines), *J. Nucl. Med.* 63 (2022) 1288–1299, <https://doi.org/10.1093/jnumed.121.263239>.
- [289] S. Ranjit, L. Malacrida, D.M. Jameson, E. Gratton, Fit-free analysis of fluorescence lifetime imaging data using the phasor approach, *Nat. Protoc.* 13 (2018) 1979–2004, <https://doi.org/10.1038/s41596-018-0026-5>.
- [290] C. Stringer, T. Wang, M. Michaelos, M. Pachitariu, Cellpose: a generalist algorithm for cellular segmentation, *Nat. Methods* 18 (2021) 100–106, <https://doi.org/10.1038/s41592-020-01018-x>.
- [291] J. Zhang, et al., Fully automated echocardiogram interpretation in clinical practice: feasibility and diagnostic accuracy, *Circulation* 138 (2018) 1623–1635, <https://doi.org/10.1161/CIRCULATIONAHA.118.034338>.
- [292] S.G. Adie, B.W. Graf, A. Ahmad, P.S. Carney, S.A. Boppart, Computational adaptive optics for broadband optical interferometric tomography of biological tissue, *Proc. Natl. Acad. Sci. USA* 109 (2012) 7175–7180, <https://doi.org/10.1073/pnas.1121193109>.
- [293] X. Chen, M.R. Lowerison, Z. Dong, A. Han, P. Song, Deep learning-based microbubble localization for ultrasound localization microscopy, *IEEE Trans. Ultrason., Ferroelectr., Freq. Contr.* 69 (2022) 1312–1325, <https://doi.org/10.1109/TUFFC.2022.3152225>.
- [294] H. Jang, et al., Super-resolution SRS microscopy with A-PoD, *Nat. Methods* 20 (2023) 448–458, <https://doi.org/10.1038/s41592-023-01779-1>.
- [295] X. Peng, B.P. Sutton, F. Lam, Z. Liang, DeepSENSE: learning coil sensitivity functions for SENSE reconstruction using deep learning, *Magnetic Resonance in Med* 87 (2022) 1894–1902, <https://doi.org/10.1002/mrm.29085>.
- [296] A. Speiser, et al., Deep learning enables fast and dense single-molecule localization with high accuracy, *Nat. Methods* 18 (2021) 1082–1090, <https://doi.org/10.1038/s41592-021-01236-x>.
- [297] A. Ghaffarizadeh, S.H. Friedman, P. Macklin, BioFVM: an efficient, parallelized diffusive transport solver for 3-D biological simulations, *Bioinformatics* 32 (2016) 1256–1258, <https://doi.org/10.1093/bioinformatics/btv730>.
- [298] A. Ghaffarizadeh, R. Heiland, S.H. Friedman, S.M. Mumenthaler, P. Macklin, PhysCell: an open source physics-based cell simulator for 3-D multicellular systems, *PLoS Comput. Biol.* 14 (2018) e1005991, <https://doi.org/10.1371/journal.pcbi.1005991>.
- [299] C.M. Glen, M.L. Kemp, E.O. Voit, Agent-based modeling of morphogenetic systems: advantages and challenges, *PLoS Comput. Biol.* 15 (2019) e1006577, <https://doi.org/10.1371/journal.pcbi.1006577>.
- [300] A. Plić, H. Lapp, The PLOS computational biology software section, *PLoS Comput. Biol.* 8 (2012) e1002799, <https://doi.org/10.1371/journal.pcbi.1002799>.
- [301] A.P. Alivisatos, M. Chun, G.M. Church, R.J. Greenspan, M.L. Roukes, R. Yuste, The brain activity map project and the challenge of functional connectomics, *Neuron* 74 (2012) 970–974, <https://doi.org/10.1016/j.neuron.2012.06.006>.
- [302] A. Dräger, et al., SysMod: the ISCB community for data-driven computational modelling and multi-scale analysis of biological systems, *Bioinformatics* 37 (2021) 3702–3706, <https://doi.org/10.1093/bioinformatics/btab229>.
- [303] HuBMAP Consortium, et al., The human body at cellular resolution: the NIH Human Biomolecular Atlas Program, *Nature* 574 (2019) 187–192, <https://doi.org/10.1038/s41586-019-1629-x>.
- [304] L. Pantanowitz, A. Sharma, A.B. Carter, T. Kurc, A. Sussman, J. Saltz, Twenty years of digital pathology: an overview of the road travelled, what is on the horizon, and the emergence of vendor-neutral archives, *J. Pathol. Inf.* 9 (2018) 40, https://doi.org/10.4103/jpi.jpi_69_18.
- [305] M.N. Gurcan, L.E. Boucheron, A. Can, A. Madabhushi, N.M. Rajpoot, B. Yener, Histopathological image analysis: a review, *IEEE Rev. Biomed. Eng.* 2 (2009) 147–171, <https://doi.org/10.1109/RBME.2009.2034865>.
- [306] C. Hu, S. He, Y.J. Lee, Y. He, E.M. Kong, H. Li, M.A. Anastasio, G. Popescu, Live-dead assay on unlabeled cells using phase imaging with computational specificity, *Nat. Commun.* 13 (2022) 713, <https://doi.org/10.1038/s41467-022-28214-x>.
- [307] S. Banerji, S. Mitra, Deep learning in histopathology: a review, *WIREs Data Min & Knowl* 12 (2022), <https://doi.org/10.1002/widm.1439>.
- [308] O. Ciga, T. Xu, A.L. Martel, Self supervised contrastive learning for digital histopathology, *Machine Learning with Applications* 7 (2022) 100198, <https://doi.org/10.1016/j.mlwa.2021.100198>.
- [309] A. Golatkar, D. Anand, A. Sethi, Classification of breast cancer histology using deep learning, in: A. Campilho, F. Karray, B. Ter Haar Romeny (Eds.), *Image Analysis and Recognition*, Springer International Publishing, Cham, 2018, pp. 837–844, https://doi.org/10.1007/978-3-319-93000-8_95.
- [310] O. Ronneberger, P. Fischer, T. Brox, U-net: convolutional networks for biomedical image segmentation, in: N. Navab, J. Hornegger, W.M. Wells, A.F. Frangi (Eds.), *Medical Image Computing and Computer-Assisted Intervention – MICCAI 2015*, Springer International Publishing, Cham, 2015, pp. 234–241, https://doi.org/10.1007/978-3-319-24574-4_28.
- [311] S. Olson, A.S. Downey, *Sharing Clinical Research Data: Workshop Summary*, The National Academies Press, Washington, D.C., 2013.
- [312] J.E. Sorrells, R.R. Iyer, L. Yang, A.J. Bower, D.R. Spillman, E.J. Chaney, H. Tu, S.A. Boppart, Real-time pixelwise phasor analysis for video-rate two-photon fluorescence lifetime imaging microscopy, *Biomed. Opt Express* 12 (2021) 4003–4019, <https://doi.org/10.1364/boe.424533>.
- [313] S.C. Warren, et al., Rapid global fitting of large fluorescence lifetime imaging microscopy datasets, *PLoS One* 8 (2013) e70687, <https://doi.org/10.1371/journal.pone.0070687>.
- [314] A.E. Carpenter, et al., CellProfiler: image analysis software for identifying and quantifying cell phenotypes, *Genome Biol.* 7 (2006) R100, <https://doi.org/10.1186/gb-2006-7-10-r100>.
- [315] S. You, Y. Sun, L. Yang, J. Park, H. Tu, M. Marjanovic, S. Sinha, S.A. Boppart, Real-time intraoperative diagnosis by deep neural network driven multiphoton virtual histology, *npj Precis. Oncol.* 3 (2019) 33, <https://doi.org/10.1038/s41698-019-0104-3>.
- [316] J. Metzcar, Y. Wang, R. Heiland, P. Macklin, A review of cell-based computational modeling in cancer biology, *JCO Clinical Cancer Informatics* (2019) 1–13, <https://doi.org/10.1200/CCI.18.00069>.
- [317] Y. Jiao, S. Torquato, Emergent behaviors from a cellular automaton model for invasive tumor growth in heterogeneous microenvironments, *PLoS Comput. Biol.* 7 (2011) e1002314, <https://doi.org/10.1371/journal.pcbi.1002314>.
- [318] X. Li, M.K. Jolly, J.T. George, K.J. Pienta, H. Levine, Computational modeling of the crosstalk between macrophage polarization and tumor cell plasticity in the tumor microenvironment, *Front. Oncol.* 9 (2019) 10, <https://doi.org/10.3389/fonc.2019.00010>.

- [319] J. Poleszczuk, H. Enderling, A high-performance cellular automaton model of tumor growth with dynamically growing domains, *Appl. Math.* 5 (2014) 144–152, <https://doi.org/10.4236/am.2014.51017>.
- [320] J.F. Eichinger, M.J. Grill, I.D. Kermani, R.C. Aydin, W.A. Wall, J.D. Humphrey, C.J. Cyron, A computational framework for modeling cell–matrix interactions in soft biological tissues, *Biomech. Model. Mechanobiol.* 20 (2021) 1851–1870, <https://doi.org/10.1007/s10237-021-01480-2>.
- [321] P. Vempati, F. Mac Gabhann, A.S. Popel, Quantifying the proteolytic release of extracellular matrix-sequestered VEGF with a computational model, *PLoS One* 5 (2010) e11860, <https://doi.org/10.1371/journal.pone.0011860>.
- [322] V. Cristini, J. Lowengrub, *Multiscale Modeling of Cancer: an Integrated Experimental and Mathematical Modeling Approach*, first ed., Cambridge University Press, 2010 <https://doi.org/10.1017/CBO9780511781452>.
- [323] F. Graner, J.A. Glazier, Simulation of biological cell sorting using a two-dimensional extended Potts model, *Phys. Rev. Lett.* 69 (1992) 2013–2016, <https://doi.org/10.1103/PhysRevLett.69.2013>.
- [324] H.B. Frieboes, J.S. Lowengrub, S. Wise, X. Zheng, P. Macklin, E.L. Bearer, V. Cristini, Computer simulation of glioma growth and morphology, *Neuroimage* 37 (2007) S59–S70, <https://doi.org/10.1016/j.neuroimage.2007.03.008>.
- [325] J. Tang, H. Enderling, S. Becker-Weimann, C. Pham, A. Polyzos, C.-Y. Chen, S.V. Costes, Phenotypic transition maps of 3D breast acini obtained by imaging-guided agent-based modeling, *Integr. Biol.* 3 (2011) 408, <https://doi.org/10.1039/c0ib00092b>.
- [326] T.R. Insel, S.C. Landis, F.S. Collins, Research priorities. The NIH BRAIN initiative, *Science* 340 (2013) 687–688, <https://doi.org/10.1126/science.1239276>.
- [327] International Human Genome Sequencing Consortium, et al., Initial sequencing and analysis of the human genome, *Nature* 409 (2001) 860–921, <https://doi.org/10.1038/35057062>.
- [328] V. Emiliani, A.E. Cohen, K. Deisseroth, M. Häusser, All-optical interrogation of neural circuits, *J. Neurosci.* 35 (2015) 13917–13926, <https://doi.org/10.1523/JNEUROSCI.2916-15.2015>.
- [329] C.K. Kim, A. Adhikari, K. Deisseroth, Integration of optogenetics with complementary methodologies in systems neuroscience, *Nat. Rev. Neurosci.* 18 (2017) 222–235, <https://doi.org/10.1038/nrn.2017.15>.
- [330] M. Inoue, et al., Rational design of a high-affinity, fast, red calcium indicator R-CaMP2, *Nat. Methods* 12 (2015) 64–70, <https://doi.org/10.1038/nmeth.3185>.
- [331] A. Perron, H. Mutoh, T. Launey, T. Knöpfel, Red-shifted voltage-sensitive fluorescent proteins, *Chem. Biol.* 16 (2009) 1268–1277, <https://doi.org/10.1016/j.chembiol.2009.11.014>.
- [332] O.M. Subach, F.V. Subach, GAF-CaMP3–sfGFP, an enhanced version of the near-infrared genetically encoded positive phytochrome-based calcium indicator for the visualization of neuronal activity, *IJMS* 21 (2020) 6883, <https://doi.org/10.3390/ijms21186883>.
- [333] B. Yi, B.E. Kang, S. Lee, S. Braubach, B.J. Baker, A dimeric fluorescent protein yields a bright, red-shifted GEVI capable of population signals in brain slice, *Sci. Rep.* 8 (2018) 15199, <https://doi.org/10.1038/s41598-018-33297-y>.
- [334] Y. Zhao, et al., An expanded palette of genetically encoded Ca²⁺ indicators, *Science* 333 (2011) 1888–1891, <https://doi.org/10.1126/science.1208592>.
- [335] W. Akemann, M. Sasaki, H. Mutoh, T. Imamura, N. Honkura, T. Knöpfel, Two-photon voltage imaging using a genetically encoded voltage indicator, *Sci. Rep.* 3 (2013) 2231, <https://doi.org/10.1038/srep02231>.
- [336] A. Birkner, C.H. Tischbirek, A. Konnerth, Improved deep two-photon calcium imaging in vivo, *Cell Calcium* 64 (2017) 29–35, <https://doi.org/10.1016/j.ceca.2016.12.005>.
- [337] S. Chamberland, et al., Fast two-photon imaging of subcellular voltage dynamics in neuronal tissue with genetically encoded indicators, *Elife* 6 (2017) e25690, <https://doi.org/10.7554/eLife.25690>.
- [338] V. Villette, et al., Ultrafast two-photon imaging of a high-gain voltage indicator in awake behaving mice, *Cell* 179 (2019) 1590–1608.e23, <https://doi.org/10.1016/j.cell.2019.11.004>.
- [339] F. Helmchen, M.S. Fee, D.W. Tank, W. Denk, A miniature head-mounted two-photon microscope, *Neuron* 31 (2001) 903–912, [https://doi.org/10.1016/S0896-6273\(01\)00421-4](https://doi.org/10.1016/S0896-6273(01)00421-4).
- [340] A. Li, H. Guan, H.-C. Park, Y. Yue, D. Chen, W. Liang, M.-J. Li, H. Lu, X. Li, Twist-free ultralight two-photon fiberscope enabling neuroimaging on freely rotating/walking mice, *Optica* 8 (2021) 870, <https://doi.org/10.1364/OPTICA.422657>.
- [341] C. Tischbirek, A. Birkner, H. Jia, B. Sakmann, A. Konnerth, Deep two-photon brain imaging with a red-shifted fluorometric Ca²⁺ indicator, *Proc. Natl. Acad. Sci. U.S.A.* 112 (2015) 11377–11382, <https://doi.org/10.1073/pnas.1514209112>.
- [342] E. Papagiakoumou, A. Bégue, B. Leshem, O. Schwartz, B.M. Stell, J. Bradley, D. Oron, V. Emiliani, Functional patterned multiphoton excitation deep inside scattering tissue, *Nature Photon* 7 (2013) 274–278, <https://doi.org/10.1038/nphoton.2013.9>.
- [343] C. Lavigne, P. Brumer, Pulsed two-photon coherent control of channelrhodopsin-2 photocurrent in live brain cells, *J. Chem. Phys.* 153 (2020) 034303, <https://doi.org/10.1063/5.0012642>.
- [344] K. Paul, P. Sengupta, E.D. Ark, H. Tu, Y. Zhao, S.A. Boppart, Coherent control of an opsin in living brain tissue, *Nature Phys* 13 (2017) 1111–1116, <https://doi.org/10.1038/nphys4257>.
- [345] N.C. Klapoetke, et al., Independent optical excitation of distinct neural populations, *Nat. Methods* 11 (2014) 338–346, <https://doi.org/10.1038/nmeth.2836>.
- [346] J.Y. Lin, P.M. Knutsen, A. Müller, D. Kleinfeld, R.Y. Tsien, ReaChR: a red-shifted variant of channelrhodopsin enables deep transcranial optogenetic excitation, *Nat. Neurosci.* 16 (2013) 1499–1508, <https://doi.org/10.1038/nn.3502>.
- [347] A.R. Mardinly, I.A. Oldenburg, N.C. Pégard, S. Sridharan, E.H. Lyall, K. Chesnov, S.G. Brohawn, L. Waller, H. Adesnik, Precise multimodal optical control of neural ensemble activity, *Nat. Neurosci.* 21 (2018) 881–893, <https://doi.org/10.1038/s41593-018-0139-8>.
- [348] J.P. Rickgauer, D.W. Tank, Two-photon excitation of channelrhodopsin-2 at saturation, *Proc. Natl. Acad. Sci. U.S.A.* 106 (2009) 15025–15030, <https://doi.org/10.1073/pnas.0907084106>.
- [349] N.C. Pégard, A.R. Mardinly, I.A. Oldenburg, S. Sridharan, L. Waller, H. Adesnik, Three-dimensional scanless holographic optogenetics with temporal focusing (3D-SHOT), *Nat. Commun.* 8 (2017) 1228, <https://doi.org/10.1038/s41467-017-01031-3>.
- [350] S.L. Farhi, et al., Wide-area all-optical neurophysiology in acute brain slices, *J. Neurosci.* 39 (2019) 4889–4908, <https://doi.org/10.1523/JNEUROSCI.0168-19.2019>.
- [351] F. Gobbo, et al., Activity-dependent expression of Channelrhodopsin at neuronal synapses, *Nat. Commun.* 8 (2017) 1629, <https://doi.org/10.1038/s41467-017-01699-7>.
- [352] K.V. Kastanenka, R. Moreno-Bote, M. De Pittà, G. Perea, A. Eraso-Pichot, R. Masgrau, K.E. Poskanzer, E. Galea, A roadmap to integrate astrocytes into Systems Neuroscience, *Glia* 68 (2020) 5–26, <https://doi.org/10.1002/glia.23632>.
- [353] D. Barata, C. Van Blitterswijk, P. Habibovic, High-throughput screening approaches and combinatorial development of biomaterials using microfluidics, *Acta Biomater.* 34 (2016) 1–20, <https://doi.org/10.1016/j.actbio.2015.09.009>.
- [354] A. Carnero, High throughput screening in drug discovery, *Clin. Transl. Oncol.* 8 (2006) 482–490, <https://doi.org/10.1007/s12094-006-0048-2>.
- [355] L.M. Mayr, D. Bojanic, Novel trends in high-throughput screening, *Curr. Opin. Pharmacol.* 9 (2009) 580–588, <https://doi.org/10.1016/j.coph.2009.08.004>.
- [356] A. Schuhmacher, L. Wilisch, M. Kuss, A. Kandelbauer, M. Hinder, O. Gassmann, R&D efficiency of leading pharmaceutical companies – a 20-year analysis, *Drug Discov. Today* 26 (2021) 1784–1789, <https://doi.org/10.1016/j.drudis.2021.05.005>.
- [357] D.W. Lee, I. Doh, D.-H. Nam, Unified 2D and 3D cell-based high-throughput screening platform using a micropillar/microwell chip, *Sensor. Actuator. B Chem.* 228 (2016) 523–528, <https://doi.org/10.1016/j.snb.2016.01.011>.
- [358] W. Lim, S. Park, A microfluidic spheroid culture device with a concentration gradient generator for high-throughput screening of drug efficacy, *Molecules* 23 (2018) 3355, <https://doi.org/10.3390/molecules23123355>.
- [359] P. Baillargeon, J. Shumate, S. Hou, V. Fernandez-Vega, N. Marques, G. Souza, J. Seldin, T.P. Spicer, L. Scampavia, Automating a magnetic 3D spheroid model technology for high-throughput screening, *SLAS Technology* 24 (2019) 420–428, <https://doi.org/10.1177/2472630319854337>.
- [360] S. Peel, et al., Introducing an automated high content confocal imaging approach for Organs-on-Chips, *Lab Chip* 19 (2019) 410–421, <https://doi.org/10.1039/C8LC00829A>.

- [361] S.J. Kochanek, D.A. Close, P.A. Johnston, High content screening characterization of head and neck squamous cell carcinoma multicellular tumor spheroid cultures generated in 384-well ultra-low attachment plates to screen for better cancer drug leads, *Assay Drug Dev. Technol.* 17 (2019) 17–36, <https://doi.org/10.1089/adt.2018.896>.
- [362] P. Chen, et al., Patient-derived organoids can guide personalized-therapies for patients with advanced breast cancer, *Adv. Sci.* 8 (2021) 2101176, <https://doi.org/10.1002/advs.202101176>.
- [363] H.H.-F. Loong, et al., Patient-derived tumor organoid predicts drugs response in glioblastoma: a step forward in personalized cancer therapy? *J. Clin. Neurosci.* 78 (2020) 400–402, <https://doi.org/10.1016/j.jocn.2020.04.107>.
- [364] E. Driehuis, et al., Pancreatic cancer organoids recapitulate disease and allow personalized drug screening, *Proc. Natl. Acad. Sci. U.S.A.* 116 (2019) 26580–26590, <https://doi.org/10.1073/pnas.1911273116>.
- [365] J. Kondo, M. Inoue, Application of cancer organoid model for drug screening and personalized therapy, *Cells* 8 (2019) 470, <https://doi.org/10.3390/cells8050470>.
- [366] Z. Dantes, et al., Implementing cell-free DNA of pancreatic cancer patient-derived organoids for personalized oncology, *JCI Insight* 5 (2020) e137809, <https://doi.org/10.1172/jci.insight.137809>.
- [367] P. Schneider, et al., Rethinking drug design in the artificial intelligence era, *Nat. Rev. Drug Discov.* 19 (2020) 353–364, <https://doi.org/10.1038/s41573-019-0050-3>.
- [368] J. Vamathevan, et al., Applications of machine learning in drug discovery and development, *Nat. Rev. Drug Discov.* 18 (2019) 463–477, <https://doi.org/10.1038/s41573-019-0024-5>.